Supporting Information for:

A redox-switchable catalyst with an 'unplugged' redox tag

Cristian Gutiérrez-Peña, Macarena Poyatos and Eduardo Peris**

Institute of Advanced Materials (INAM). Universitat Jaume I. Av. Vicente Sos Baynat s/n. Castellón. E-12071. Spain. Email: eperis@uji.es, poyatosd@uji.es

General considerations

N,N'-Bis(3-propylimidazole)-1,4,5,8-naphthalenediimide (**I**),[1] N,N'-bis(1-*n*-butyl-3-propylimidazolium)-1,4,5,8-naphthalenediimide ([**1A**](Br)$_2$)[2] and N,N'-bis(1-benzyl-3-propylimidazolium)-1,4,5,8-naphthalenediimide ([**1B**](Br)$_2$)[2] were prepared as described in the literature. All the other reagents were used as received from the commercial suppliers. Anhydrous solvents were dried using a solvent purification system (SPS M BRAUN) or purchased and degassed prior to use by purging them with dry argon or nitrogen. Column chromatography was performed using silica gel (60-120 mesh). NMR spectra were recorded on a Bruker 400 or 300 MHz, chemical shifts (δ) are expressed in ppm using the residual proton resonance of the solvent as an internal standard. All coupling constants (*J*) are expressed in hertz (Hz). Signals marked with an asterisk (*) in the NMR spectra correspond to Apiezon brand H grease.[3] Infrared spectra (FTIR) were performed on a Bruker Equinox 55 spectrometer with a spectral window of 4000-400 cm^{-1}. Mass spectra (ESI-MS) were collected from *m/z* 0 – 1500 in Micromass Quatro LC instrument. UV-Visible absorption spectra were recorded on a Varian Cary 300 BIO spectrophotometer using dry and degassed CH_2Cl_2 under ambient conditions. Emission spectra were recorded on a modular Horiba FluoroLog-3 spectrofluorometer employing CH_2Cl_2.

1. Synthesis and characterization of compounds

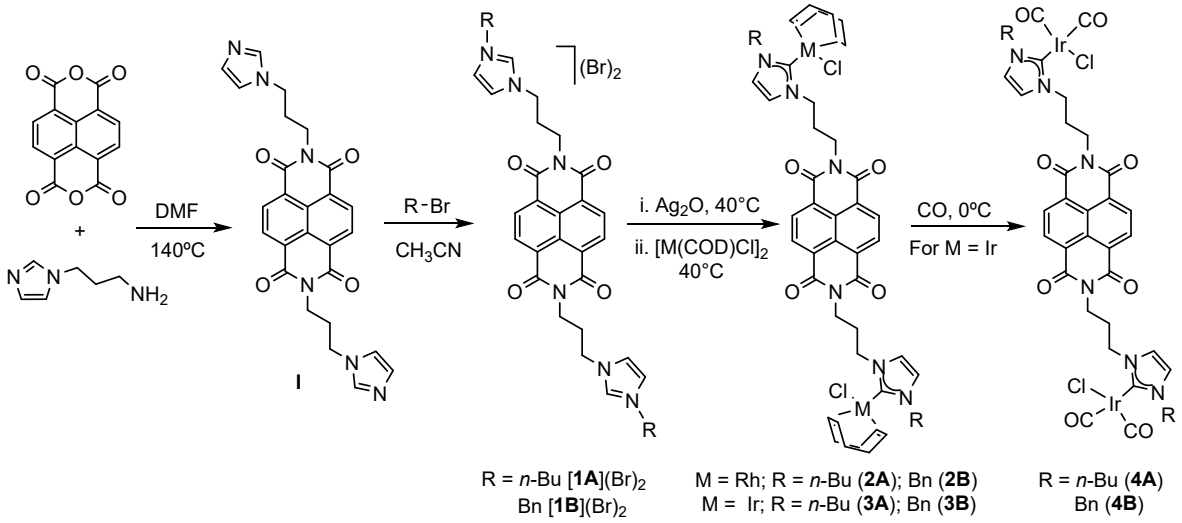

Scheme S1. Synthesis of NDI-NHC complexes **2**-**4**

General procedure for the synthesis of NDI-NHC complexes 2 and 3. Silver oxide (1.2 equiv.) was added to a solution of the corresponding NDI-bis-imidazolium salt ([**1A**]$(Br)_2$ or ([**1B**]$(Br)_2$) (1 equiv.) in dichloromethane (100 mL). The mixture was stirred at 40°C overnight. After this time, $[M(COD)Cl]_2$ (M = Rh or Ir, 1 equiv.) was added to the resulting suspension. The mixture was stirred at 40°C for 4 hours and filtered through Celite. The solvent was removed under vacuum and the crude product was purified by column chromatography using dichloromethane and dichloromethane/acetone mixtures as eluent.

Synthesis and characterization of 2A. Complex **2A** was prepared employing the general procedure by reacting bis-imidazolium salt [**1A**]$(Br)_2$ (100 mg, 0.132 mmol), Ag_2O (36.8 mg, 0.159 mmol) and $[RhCl(COD)]_2$ (65.2 mg, 0.132 mmol). Complex **2A** was isolated as a dark-yellow solid in 91% yield (131 mg). ^{1}H NMR (400 MHz, $CDCl_3$): δ 8.69 (s, 4H, CH_{NDI}), 6.98-6.94 (m, 2H, CH_{imid}), 6.83-6.80 (m, 2H, CH_{imid}), 4.93-4.74 (m, 4H; 2H CH_{cod} and 2H, $N_{NDI}CH_2CH_2CH_2N_{imid}$), 4.53-4.33 (m, 8H; 2H CH_{cod}, 4H $NCH_2CH_2CH_2CH_3$ and 2H $N_{NDI}CH_2CH_2CH_2N_{imid}$), 4.30 (t, 4H, $^3J_{H-H}$ = 6.7 Hz, $N_{NDI}CH_2CH_2CH_2N_{imid}$), 3.32-3.09 (m, 4H, C$H_{cod}$), 2.49-2.17 (m, 12H; 4H $N_{imid}CH_2CH_2CH_2N_{NDI}$ and 8H C$H_{2\ cod}$), 1.97-1.62 (m, 12H; 8H C$H_{2\ cod}$ and 4H $NCH_2CH_2CH_2CH_3$), 1.44-1.35 (m, 4H, $NCH_2CH_2CH_2CH_3$), 0.95 (t, 6H, $^3J_{H-H}$ = 7.3 Hz, $NCH_2CH_2CH_2CH_3$). $^{13}C\{^1H\}$ NMR (101 MHz, $CDCl_3$): 182.0 (d, $^1J_{Rh-C}$ = 51.2 Hz, Rh-$C_{carbene}$), 163.0 (*C*=O), 130.9 (*C*H$_{NDI}$), 128.6 ($C_{q\ NDI}$), 126.7 ($C_{q\ NDI}$), 120.5 (*C*H$_{imid}$), 120.0 (*C*H$_{imid}$), 98.1 (d, J_{Rh-C} = 3.1 Hz, Rh-*C*H$_{cod}$), 97.7 (Rh-*C*H$_{cod}$),

68.5 (dd, J_{Rh-C} = 14.8, 3.4 Hz, Rh-*C*H$_{cod}$), 67.3 (dd, J_{Rh-C} = 14.6, 2.3 Hz, Rh-*C*H$_{cod}$), 50.5 (N*C*H$_2$CH$_2$CH$_2$CH$_3$), 48.6 (N$_{NDI}$CH$_2$CH$_2$*C*H$_2$N$_{imid}$), 38.3 (N$_{NDI}$*C*H$_2$CH$_2$CH$_2$N$_{imid}$), 33.4 (N$_{NDI}$CH$_2$*C*H$_2$CH$_2$N$_{imid}$), 33.0 (NCH$_2$*C*H$_2$CH$_2$CH$_3$), 32.4 (*C*H$_{2\ cod}$), 29.5 (*C*H$_{2\ cod}$), 29.2 (*C*H$_{2\ cod}$), 28.4 (*C*H$_{2\ cod}$), 20.0 (NCH$_2$CH$_2$*C*H$_2$CH$_3$), 13.8 (NCH$_2$CH$_2$CH$_2$*C*H$_3$). ESI-MS (20V, *m/z*): 1051.37 [M-Cl]$^+$.

Synthesis and characterization of 2B. Complex **2B** was prepared employing the general procedure by reacting bis-imidazolium salt **1B** (100 mg, 0.121 mmol), Ag_2O (33.7 mg, 0.145 mmol) and $[RhCl(COD)]_2$ (59.7 mg, 0.121 mmol). Complex **2B** was isolated as a dark-yellow solid in 85% yield (119 mg). ^{1}H NMR (300 MHz, $CDCl_3$): δ 8.77 (s, 4H, C*H*$_{NDI}$), 7.36-7.29 (m, 10H, C*H*$_{Bn}$), 6.99 (t, 2H, $^3J_{H-H}$ = 2.0 Hz, C*H*$_{imid}$), 6.68 (d, 2H, $^3J_{H-H}$ = 1.9 Hz, C*H*$_{imid}$), 5.82 (d, 2H, $^2J_{H-H}$ = 15.0 Hz, C*H*$_{2\ Bn}$), 5.65 (d, 2H, $^2J_{H-H}$ = 15.0 Hz, C*H*$_{2\ Bn}$), 4.99-4.83 (m, 4 H; 2H C*H*$_{cod}$ and 2H N$_{NDI}$CH$_2$CH$_2$C*H*$_2$N$_{imid}$), 4.64-4.46 (m, 4H; 2H C*H*$_{cod}$ and 2H N$_{NDI}$CH$_2$CH$_2$C*H*$_2$N$_{imid}$), 4.38 (t, 4H, $^3J_{H-H}$ = 6.7 Hz, N$_{NDI}$C*H*$_2$CH$_2$CH$_2$N$_{imid}$), 3.38-3.17 (m, 4H, C*H*$_{cod}$), 2.61-1.67 (m, 20H; 16H C*H*$_{2\ cod}$ and 4H N$_{NDI}$CH$_2$C*H*$_2$CH$_2$N$_{imid}$). ^{13}C{^{1}H} NMR (75 MHz, $CDCl_3$): δ 183.2 (d, $^1J_{Rh-C}$ = 51.1 Hz, Rh-*C*$_{carbene}$), 163.1 (*C*=O), 136.5 (*C*$_{q\ NDI}$), 131.1 (*C*H$_{NDI}$), 129.0 (*C*H$_{Bn}$), 128.3 (*C*H$_{Bn}$), 128.2 (*C*H$_{Bn}$), 126.8 (*C*$_{q\ NDI}$), 120.9 (*C*H$_{imid}$), 120.6 (*C*H$_{imid}$), 98.6 (d, J_{Rh-C} = 6.8 Hz, Rh-*C*H$_{cod}$), 98.4 (dd, J_{Rh-C} = 7.1, 2.3 Hz, Rh-*C*H$_{cod}$), 68.5 (dd, J_{Rh-C} = 14.4, 2.1 Hz, Rh-*C*H$_{cod}$), 68.1 (dd, J_{Rh-C} = 14.4, 2.0 Hz, Rh-*C*H$_{cod}$), 54.7 (*C*H$_{2\ Bn}$), 48.7 (N$_{NDI}$CH$_2$CH$_2$*C*H$_2$N$_{imid}$), 38.5 (N$_{NDI}$*C*H$_2$CH$_2$CH$_2$N$_{imid}$), 33.4 (*C*H$_{2\ cod}$), 32.6 (N$_{NDI}$CH$_2$*C*H$_2$CH$_2$N$_{imid}$), 29.7 (*C*H$_{2\ cod}$), 29.2 (*C*H$_{2\ cod}$), 28.7 (*C*H$_{2\ cod}$). ESI-MS (20V, *m/z*): 1119.31 [M-Cl]$^+$.

Synthesis and characterization of 3A. Complex **3A** was prepared employing the general procedure by reacting bis-imidazolium salt **1A** (100 mg, 0.132 mmol), Ag_2O (36.8 mg, 0.159 mmol) and $[IrCl(COD)]_2$ (88.7 mg, 0.132 mmol). Complex **3A** was isolated as a dark-yellow solid in 86% yield (144 mg). ^{1}H NMR (400 MHz, $CDCl_3$): δ 8.73 (s, 4H C*H*$_{NDI}$), 7.00-6.96 (m, 2H, C*H*$_{imid}$), 6.86-6.82 (m, 2H, C*H*$_{imid}$), 4.79-4.65 (m, 2H, N$_{NDI}$CH$_2$CH$_2$C*H*$_2$N$_{imid}$), 4.46-4.18 (m, 12H; 2H C*H*$_{cod}$, 2H N$_{NDI}$CH$_2$CH$_2$C*H*$_2$N$_{imid}$, 4H NC*H*$_2$CH$_2$CH$_2$CH$_3$, 4H N$_{NDI}$C*H*$_2$CH$_2$CH$_2$N$_{imid}$), 3.96-3.77 (m, 2H, C*H*$_{cod}$), 2.92-2.85 (m, 2H, C*H*$_{cod}$), 2.82-2.74 (m, 2H, C*H*$_{cod}$), 2.49-2.35 (m, 2H, C*H*$_{2\ cod}$), 2.33-2.22 (m, 2H, C*H*$_{2\ cod}$), 2.22-1.51 (m, 20 H; 12H C*H*$_{2\ cod}$, 4H N$_{NDI}$CH$_2$C*H*$_2$CH$_2$N$_{imid}$ and 4H NCH$_2$C*H*$_2$CH$_2$CH$_3$), 1.43-1.33 (m, 4H, NCH$_2$CH$_2$C*H*$_2$CH$_3$), 0.95 (t, 6H, $^3J_{H-H}$ = 8.7 Hz, NCH$_2$CH$_2$CH$_2$C*H*$_3$). ^{13}C{^{1}H} NMR (101

MHz, $CDCl_3$): δ 180.1 (Ir-$C_{carbene}$), 163.1 (C=O), 131.0 (CH_{NDI}), 126.8 ($C_{q\ NDI}$), 126.8 ($C_{q\ NDI}$), 120.3 (CH_{imid}), 119.8 (CH_{imid}), 84.4 (CH_{cod}), 83.4 (CH_{cod}), 52.2 (CH_{cod}), 50.9 (CH_{cod}), 50.3 ($NCH_2CH_2CH_2CH_3$), 48.3 ($N_{NDI}CH_2CH_2CH_2N_{imid}$), 38.3 ($N_{NDI}CH_2CH_2CH_2N_{imid}$), 34.3 ($CH_{2\ cod}$), 33.0 ($CH_{2\ cod}$), 30.2 ($CH_{2\ cod}$), 29.7 ($CH_{2\ cod}$), 22.7 ($N_{NDI}CH_2CH_2CH_2N_{imid}$), 20.0 ($NCH_2CH_2CH_2CH_3$), 13.8 ($NCH_2CH_2CH_2CH_3$). ESI-MS (20V, *m/z*): 1229.70 $[M\text{-}Cl]^+$.

Synthesis and characterization of 3B. Complex **3B** was prepared employing the general procedure by reacting bis-imidazolium salt **1B** (100 mg, 0.121 mmol), Ag_2O (33.7 mg, 0.145 mmol) and $[IrCl(COD)]_2$ (81.3 mg, 0.121 mmol). Complex **3B** was isolated as a dark-orange solid in 82% yield (133 mg). ^{1}H NMR (400 MHz, $CDCl_3$): δ 8.78 (s, 4H CH_{NDI}), 7.35-7.27 (m, 10H, CH_{Bn}), 6.99 (t, 2H, $^3J_{H\text{-}H}$ = 2.3 Hz, CH_{imid}), 6.69 (d, 2H, $^3J_{H\text{-}H}$ = 1.52 Hz, CH_{imid}), 5.72 (d, 2H, $^2J_{H\text{-}H}$ = 14.7 Hz, $CH_{2\ Bn}$), 5.48 (d, 2H, $^2J_{H\text{-}H}$ = 16.4 Hz, $CH_{2\ Bn}$), 4.84-4.71 (m, 2H, $N_{NDI}CH_2CH_2CH_2N_{imid}$), 4.50-4.25 (m, 8H; 2H $N_{NDI}CH_2CH_2CH_2N_{imid}$, 2H CH_{cod} and 4H $N_{NDI}CH_2CH_2CH_2N_{imid}$), 4.06-3.93 (m, 2H, CH_{cod}), 2.99-2.90 (m, 2H, CH_{cod}), 2.87-2.78 (m, 2H, CH_{cod}), 2.54-2.27 (m, 4H, $CH_{2\ cod}$), 2.07-1.37 (m, 16H; 4H $N_{NDI}CH_2CH_2CH_2N_{imid}$ and 12H $CH_{2\ cod}$). $^{13}C\{^1H\}$ NMR (101 MHz, $CDCl_3$): δ 180.9 (Ir-$C_{carbene}$), 163.1 (C=O), 136.4 ($C_{q\ NDI}$), 131.2 (CH_{NDI}), 129.0 (CH_{Bn}), 128.3 (CH_{Bn}), 128.2 (CH_{Bn}), 126.9 ($C_{q\ NDI}$), 126.8 ($C_{q\ Bn}$), 120.5 (CH_{imid}), 120.3 (CH_{imid}), 85.1 (CH_{cod}), 84.2 (CH_{cod}), 54.4 ($CH_{2\ Bn}$), 52.3 (CH_{cod}), 51.5 (CH_{cod}), 48.4 ($N_{NDI}CH_2CH_2CH_2N_{imid}$), 38.4 ($N_{NDI}CH_2CH_2CH_2N_{imid}$), 34.2 ($CH_{2\ cod}$), 33.1 ($CH_{2\ cod}$), 30.0 ($CH_{2\ cod}$), 29.8 ($N_{NDI}CH_2CH_2CH_2N_{imid}$), 29.1 ($CH_{2\ cod}$). ESI-MS (20V, *m/z*): 1297.04 $[M\text{-}Cl]^+$.

General procedure for the synthesis of the carbonyl derivatives 4. CO gas (1 atm) was bubbled through a solution of complexes **3A** or **3B** (15 mg) in dichloromethane (10 mL) for 45 minutes at 0ºC. A slight color change from dark yellow to light yellow was observed. The solvent was removed under reduced pressure, giving the desired carbonyl derivatives in quantitative yields.

Synthesis and characterization of 4A. Complex **4A** was isolated as a yellow-orange solid starting from complex **3A**. ^{1}H NMR (400 MHz, $CDCl_3$): δ 8.78 (s, 4H, CH_{NDI}), 7.15 (d, 2H, $^2J_{H\text{-}H}$ = 1.9 Hz, CH_{imid}), 6.99 (d, 2H, $^2J_{H\text{-}H}$ = 1.9 Hz, CH_{imid}), 4.50-4.38 (m, 4H, $N_{imid}CH_2CH_2CH_2N$), 4.35-4.24 (m, 6H; 2H $NCH_2CH_2CH_2CH_3$ and 4H $N_{NDI}CH_2CH_2CH_2N_{imid}$), 4.21-4.11 (m, 2H, $NCH_2CH_2CH_2CH_3$), 2.44-2.38 (m, 4H, $N_{NDI}CH_2CH_2CH_2N_{imid}$), 1.89-1.75 (m, 4H, $NCH_2CH_2CH_2CH_3$), 1.36 (sext, 4H, $^3J_{H\text{-}H}$ = 7.5 Hz, $NCH_2CH_2CH_2CH_3$), 0.95 (t, 6H, $^3J_{H\text{-}H}$ =

7.3 Hz, $NCH_2CH_2CH_2CH_3$). $^{13}C\{^1H\}$ (101 MHz, $CDCl_3$): δ 180.0 (Ir-$C_{carbene}$), 172.5 (Ir-*C*O), 166.9 (Ir-*C*O), 162.0 (*C*=O), 130.1 (CH_{NDI}), 127.7 ($C_{q\ NDI}$), 125.8 ($C_{q\ NDI}$), 120.2 (CH_{imid}), 120.2 (CH_{imid}), 50.2 ($NCH_2CH_2CH_2CH_3$), 48.0 ($N_{NDI}CH_2CH_2CH_2N_{imid}$), 36.8 ($N_{NDI}CH_2CH_2CH_2N_{imid}$), 31.7 ($N_{NDI}CH_2CH_2CH_2N_{imid}$), 28.4 ($NCH_2CH_2CH_2CH_3$), 18.7 ($NCH_2CH_2CH_2CH_3$), 12.6 ($NCH_2CH_2CH_2CH_3$). ESI-MS (20V, *m/z*): 1125.23 $[M\text{-}Cl]^+$. IR (CH_2Cl_2): 2002 ($\nu_{Ir\text{-}CO}$) and 2080 ($\nu_{Ir\text{-}CO}$) cm^{-1}.

Synthesis and characterization of 4B. Complex **4B** was isolated as a yellow-orange solid starting from complex **3B**. ^1H NMR (400 MHz, $CDCl_3$): δ 8.78 (s, 4H, CH_{NDI}), 7.42-7.27 (m, 10H, CH_{Bn}), 7.15 (d, 2H, $^2J_{H\text{-}H}$ = 2.0 Hz, CH_{imid}), 6.87 (d, 2H, $^2J_{H\text{-}H}$ = 2.0 Hz, CH_{imid}), 5.47 (d, 4H, $CH_{2\ Bn}$), 4.53-4.41 (4H, $N_{NDI}CH_2CH_2CH_2N_{imid}$), 4.33 (t, $^3J_{H\text{-}H}$ = 6.6 Hz, $N_{NDI}CH_2CH_2CH_2N_{imid}$), 2.46-2.39 (m, 4H, $N_{NDI}CH_2CH_2CH_2N_{imid}$). $^{13}C\{^1H\}$ NMR (101 MHz, $CDCl_3$): δ 181 (Ir-$C_{carbene}$), 174.2 (Ir-*C*O), 167.9 (Ir-*C*O), 163.2 (*C*=O), 135.3 ($C_{q\ NDI}$), 131.3 (CH_{NDI}), 129.2 (CH_{Bn}), 128.8 (CH_{Bn}), 128.7 (CH_{Bn}), 127.0 ($C_{q\ NDI}$), 126.8 ($C_{q\ Bn}$), 121.8 (CH_{imid}), 121.5 (CH_{imid}), 55.2 ($CH_{2\ Bn}$), 49.2 ($N_{NDI}CH_2CH_2CH_2N_{imid}$), 38.0 ($N_{NDI}CH_2CH_2CH_2N_{imid}$), 28.2 ($N_{NDI}CH_2CH_2CH_2N_{imid}$). ESI-MS (20V, *m/z*): 1193.17 $[M\text{-}Cl]^+$. IR (CH_2Cl_2): 1999 ($\nu_{Ir\text{-}CO}$) and 2081 ($\nu_{Ir\text{-}CO}$) cm^{-1}.

Synthesis of $[NDI\text{-}(NHC)_2][W(CO)_5]_2$

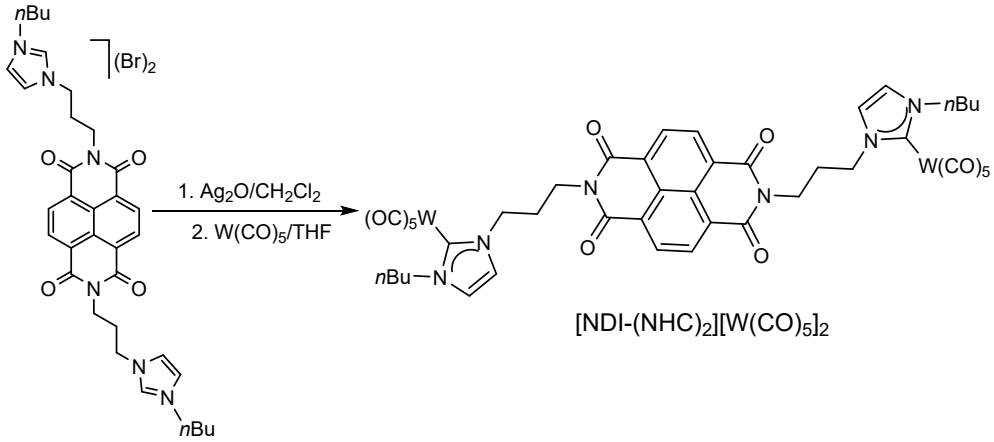

Silver oxide (28 mg, 0.12 mmol) was added to a solution of [**1A**]$(Br)_2$ (75.0 mg, 0. 1 mmol) in dichloromethane (50 mL). The mixture was stirred at 40°C overnight and then was filtered through Celite. The solvent was removed under vacuum and the crude product was dissolved in dry dichloromethane (15 mL). $W(CO)_6$ (70 mg, 0.2 mmol) and Me_3NO (15 mg, 0.2 mmol) were dissolved in THF (10 ml) and the resulting solution was stirred for 20 min. The resulting solution containing $[W(CO)_5(THF)]$ was added to the Ag-NHC solution under the exclusion

of light. The mixture was stirred at 40°C for 40 hours and filtered through Celite. The solvent was removed under vacuum and the crude product was purified by column chromatography using dichloromethane as eluent. ^{1}H NMR (300 MHz, $CDCl_3$): δ 8.78 (s, 4H, CH_{NDI}), 7.18 (d. 2H, $^{2}J_{H\text{-}H}$ = 1.98 Hz, CH_{imid}), 7.06 (d. 2H, $^{2}J_{H\text{-}H}$ = 1.98 Hz, CH_{imid}), 4.42-4.38 (m, 8H, 4H $N_{imid}CH_2CH_2$ CH_2N, 4H $NCH_2CH_2CH_2CH_3$), 4.18 (t, 4H, $^{3}J_{H\text{-}H}$ = 8.07 Hz $N_{NDI}CH_2CH_2CH_2N_{imid}$), 2.32 (q, 4H, $^{4}J_{H\text{-}H}$ = 8.01 Hz), 1.83-1.66 (m, 4H,), 1.51-1.38 (m, 4H,), 0.98 (t, 6H, $^{3}J_{H\text{-}H}$ = 8.7 Hz, $NCH_2CH_2CH_2CH_3$). $^{13}C\{^{1}H\}$ NMR ^{13}C NMR (126 MHz, $CDCl_3$) δ 201.1 (W-$C_{carbene}$), 198.3 (W-*CO*), 179.8 (W-*CO*), 163.4(C=O_{NDI}), 131.6 (C-H_{NDI}), 127.2 ($C_{q\ NDI}$), 127.0 ($C_{q\ \ NDI}$), 121.6(C-H_{imid}), 121.0 (C-H_{Imid}), 53.3 ($N_{NDI}CH_2CH_2CH_2N_{imid}$), 51.3($N_{imid}CH_2CH_2CH_2N_{NDI}$), 38.5 ($N_{imid}CH_2CH_2CH_2CH_3$), 33.8 ($N_{imid}CH_2CH_2CH_2N_{NDI}$), 33.1 ($NCH_2CH_2CH_2CH_3$), 20.33 ($NCH_2CH_2CH_2CH_3$), 14.12 ($NCH_2CH_2CH_2CH_3$).

2. Spectroscopic data

2.1 ^{1}H, $^{13}C\{^{1}H\}$ and HSQC NMR spectra of 2A in $CDCl_3$

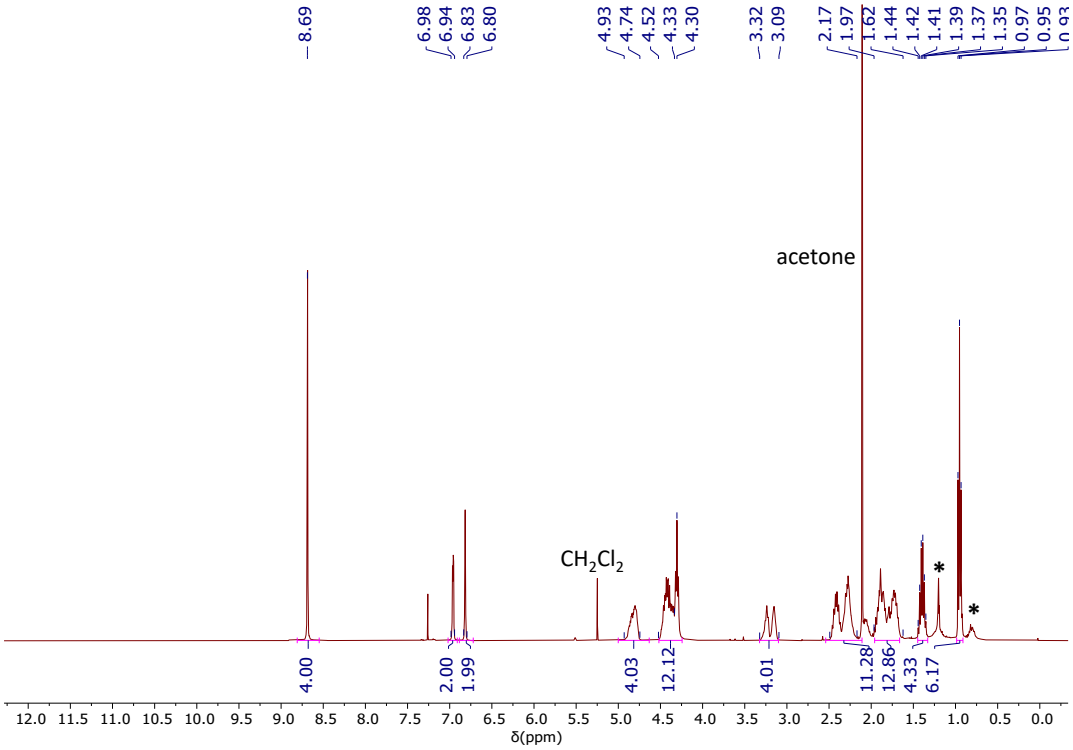

Figure S1. ^{1}H NMR spectrum (400 MHz, $CDCl_3$) of **2A**

Figure S2. $^{13}C\{^{1}H\}$ spectrum (101 MHz, $CDCl_3$) of **2A**

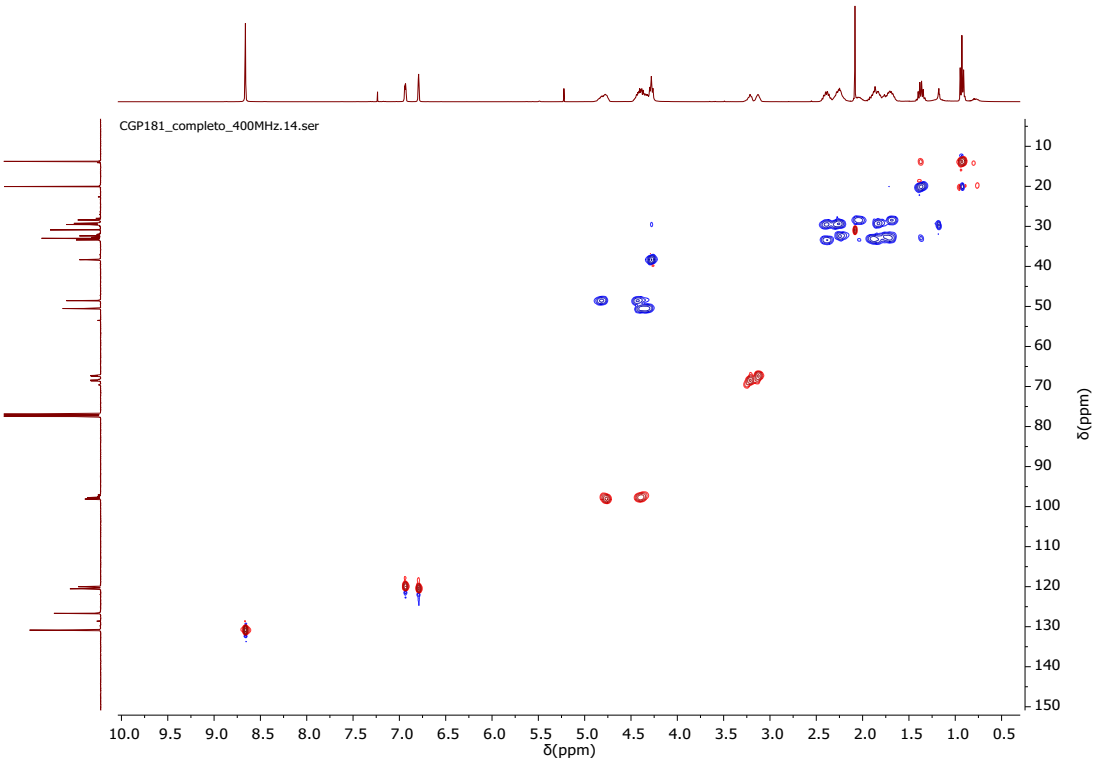

Figure S3. ^{1}H-^{13}C HSQC spectrum (400 MHz, $CDCl_3$) of **2A**

2.2 ^{1}H, $^{13}C\{^{1}H\}$ and HSQC NMR spectra of 2B in $CDCl_3$

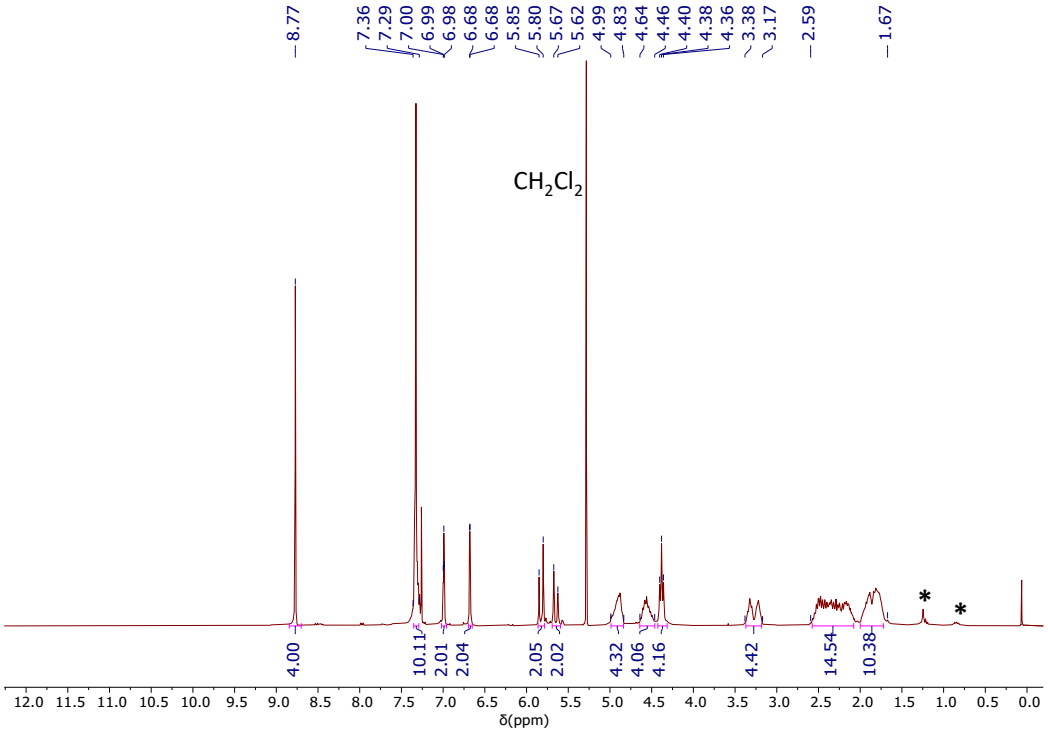

Figure S4. ^{1}H NMR spectrum (300 MHz, $CDCl_3$) of **2B**

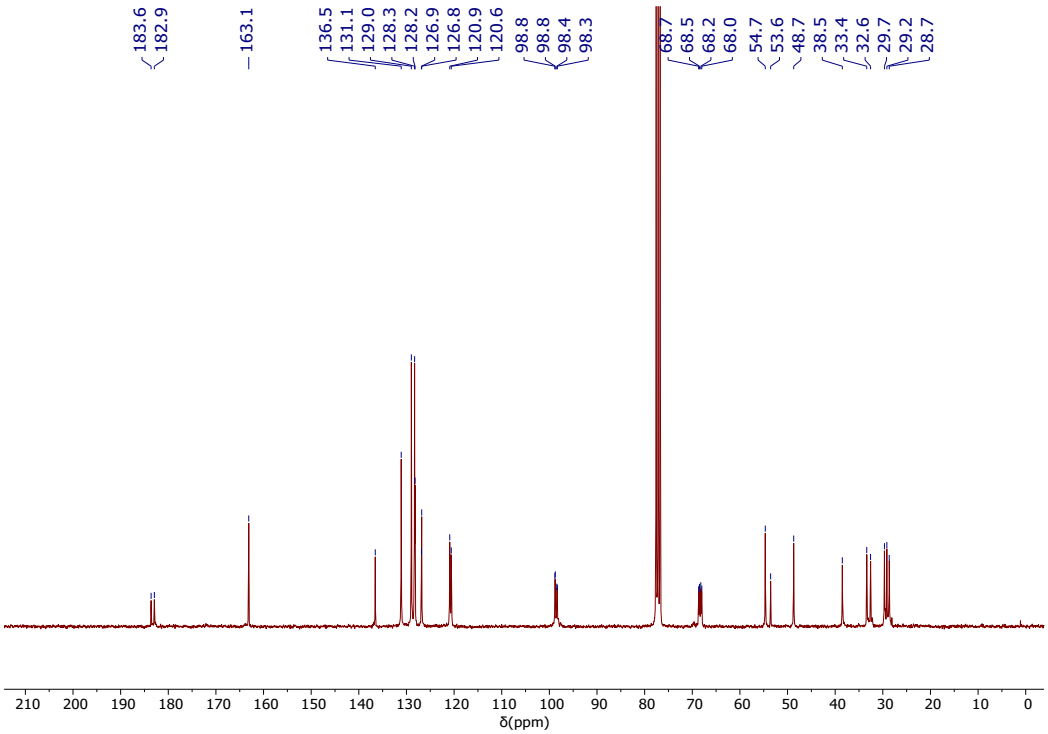

Figure S5. $^{13}C\{^{1}H\}$ spectrum (75 MHz, $CDCl_3$) of **2B**

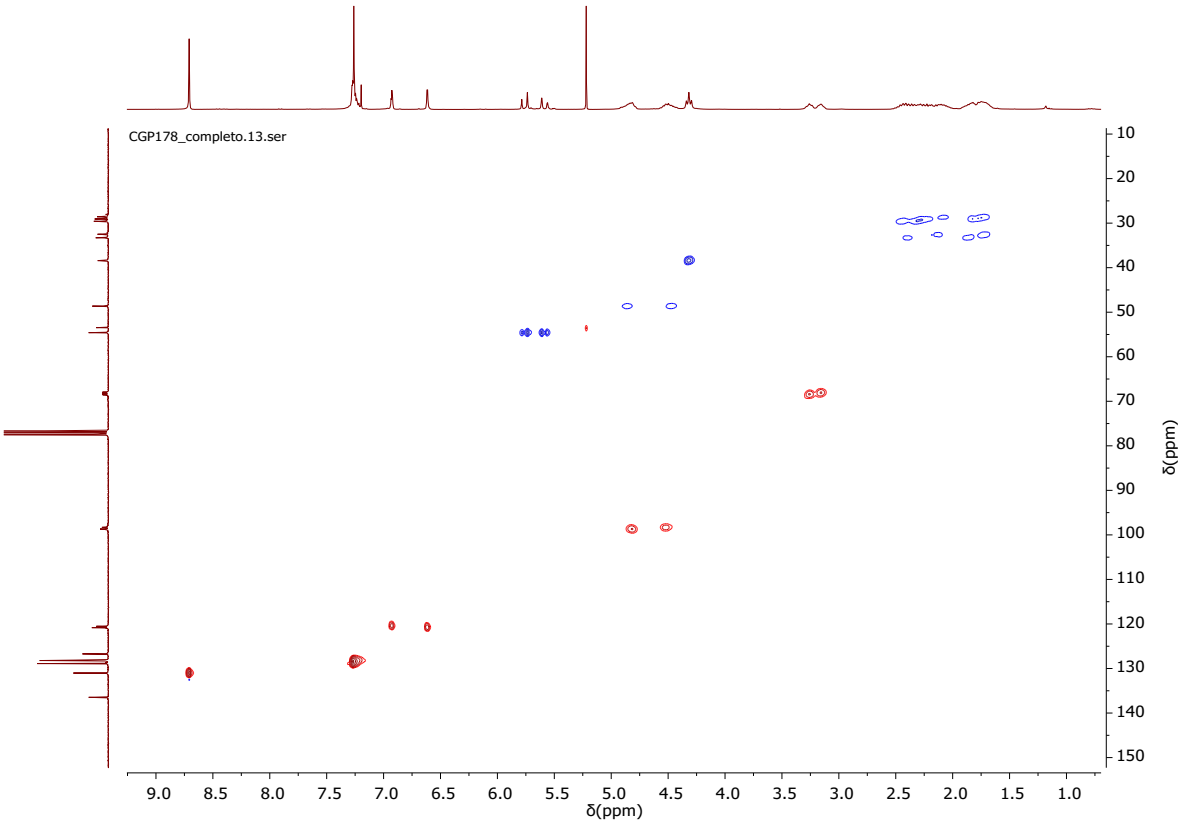

Figure S6. ^{1}H-^{13}C HSQC spectrum (400 MHz, $CDCl_3$) of **2B**

2.3 ^{1}H, $^{13}C\{^{1}H\}$ and HSQC NMR spectra of 3A in $CDCl_3$

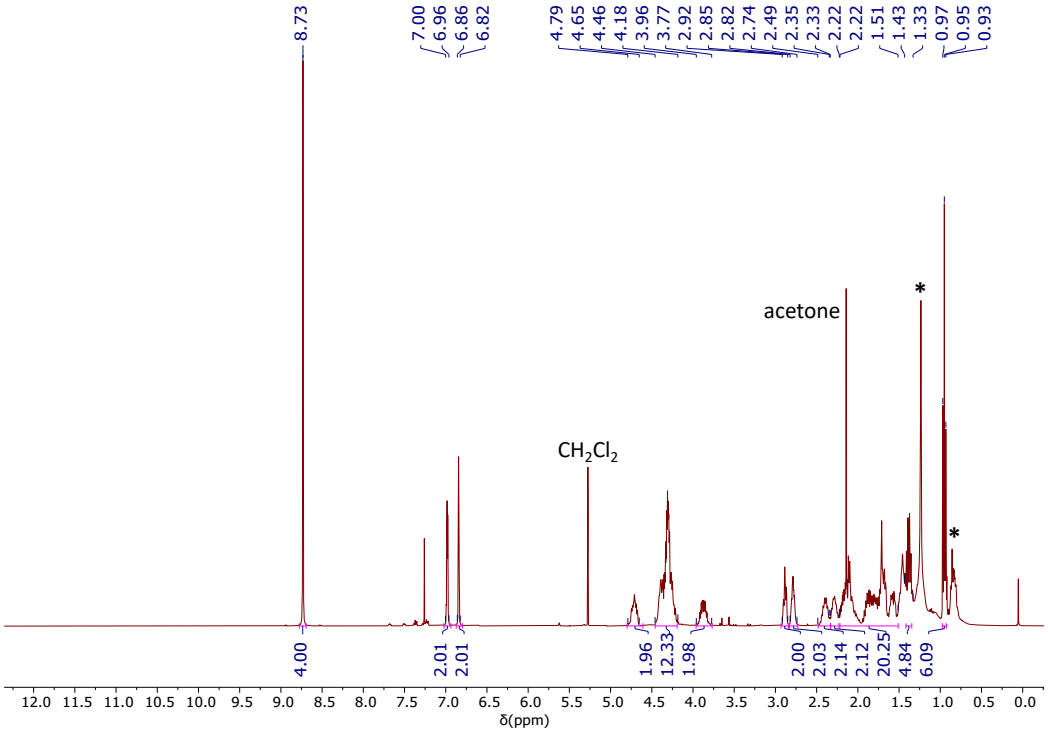

Figure S7. ^{1}H NMR spectrum (400 MHz, $CDCl_3$) of **3A**

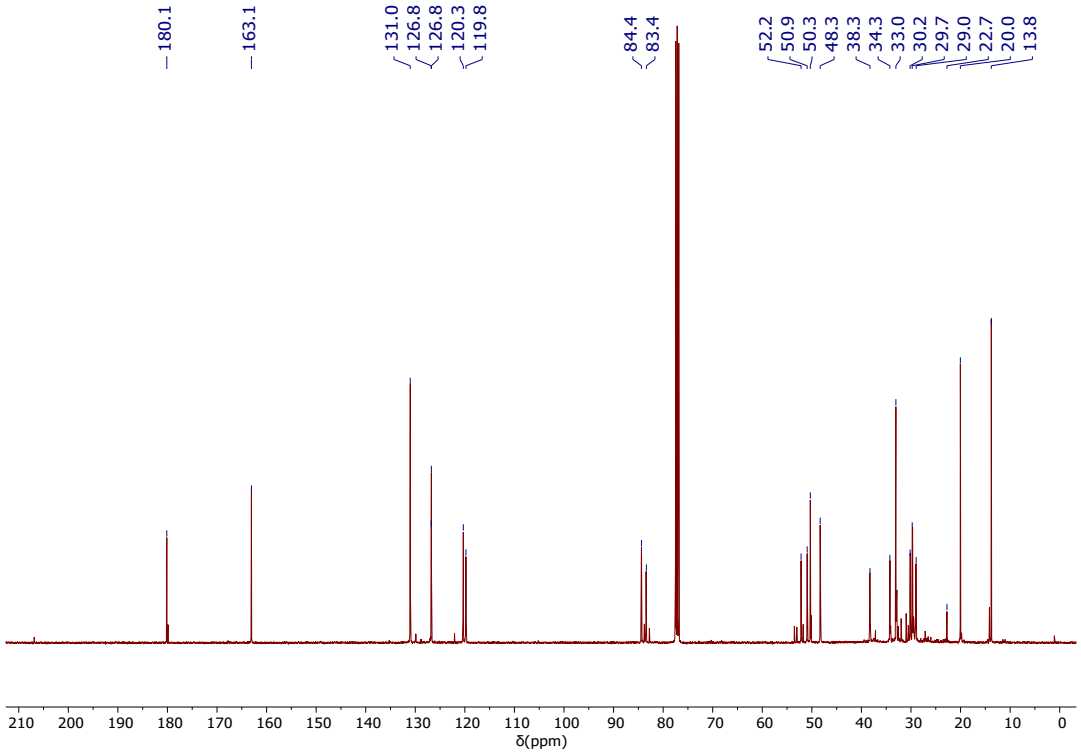

Figure S8. $^{13}C\{^{1}H\}$ spectrum (101 MHz, $CDCl_3$) of **3A**

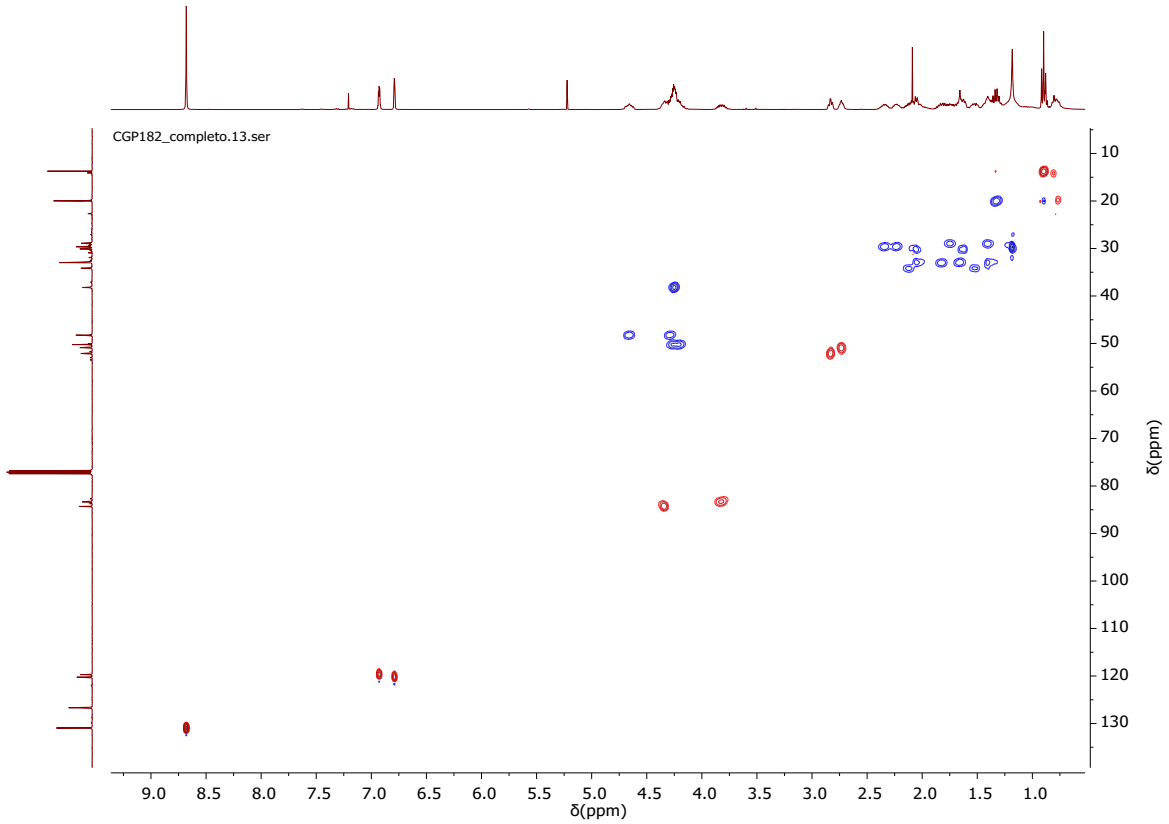

Figure S9. ^{1}H-^{13}C HSQC spectrum (400 MHz, $CDCl_3$) of **3A**

2.4 ^{1}H, $^{13}C\{^{1}H\}$ and HSQC NMR spectra of 3B in $CDCl_3$

Figure S10. ^{1}H NMR spectrum (400 MHz, $CDCl_3$) of **3B**

Figure S11. $^{13}C\{^{1}H\}$ spectrum (101 MHz, $CDCl_3$) of **3B**

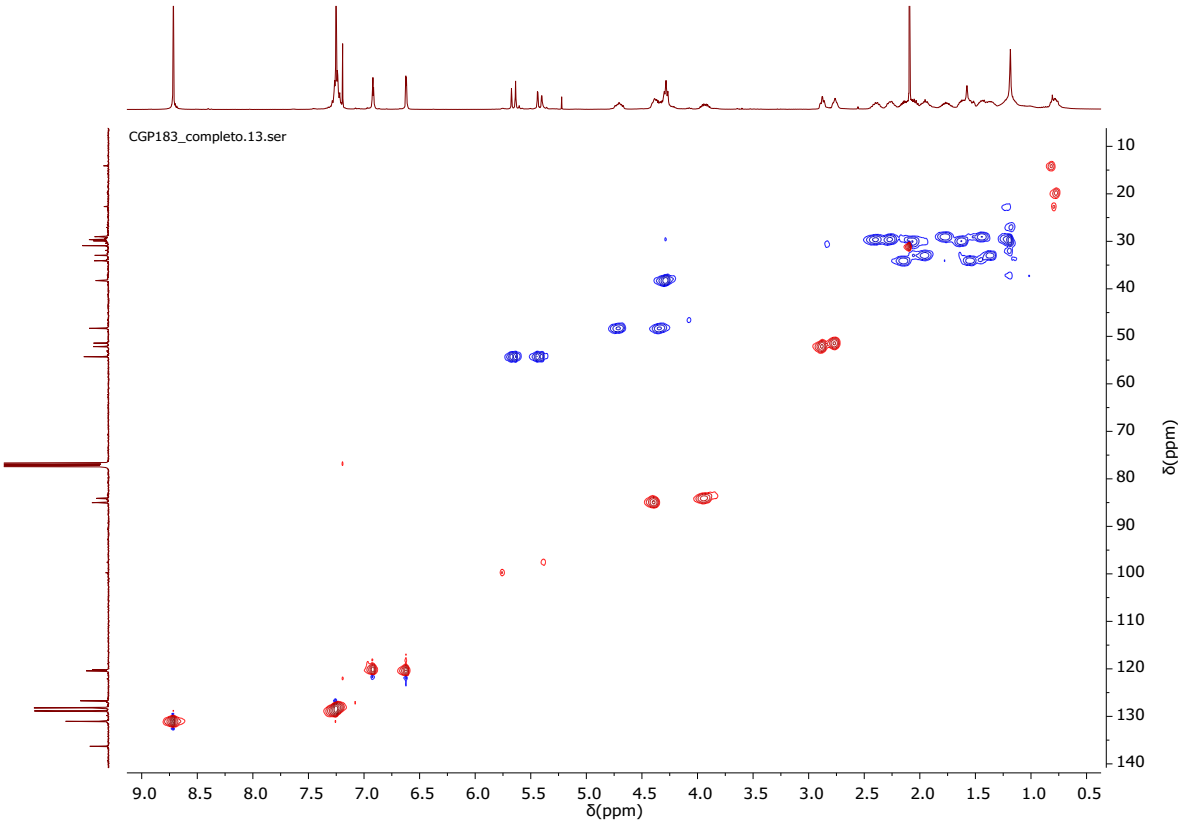

Figure S12. ^{1}H-^{13}C HSQC spectrum (400 MHz, $CDCl_3$) of **3B**

2.5 ^{1}H, $^{13}C\{^{1}H\}$ NMR spectra of 4A in $CDCl_3$

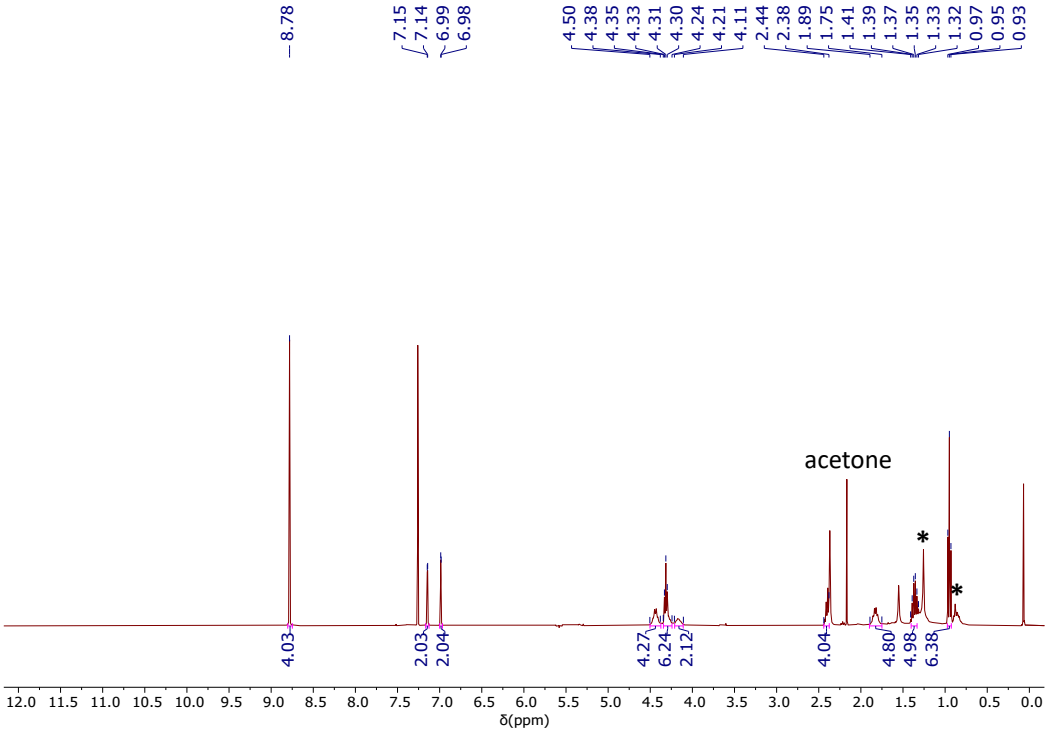

Figure S13. ^{1}H NMR spectrum (400 MHz, $CDCl_3$) of **4A**

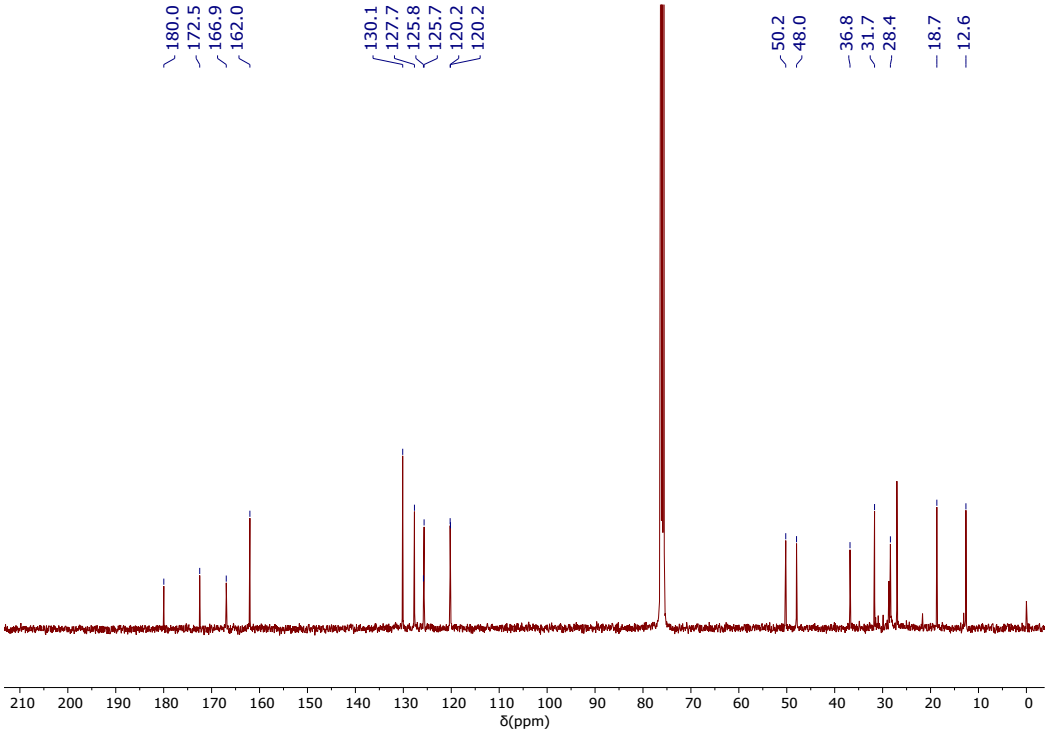

Figure S14. $^{13}C\{^{1}H\}$ spectrum (101 MHz, $CDCl_3$) of **4A**

2.6 ^{1}H, $^{13}C\{^{1}H\}$ NMR spectra of 4B in $CDCl_3$

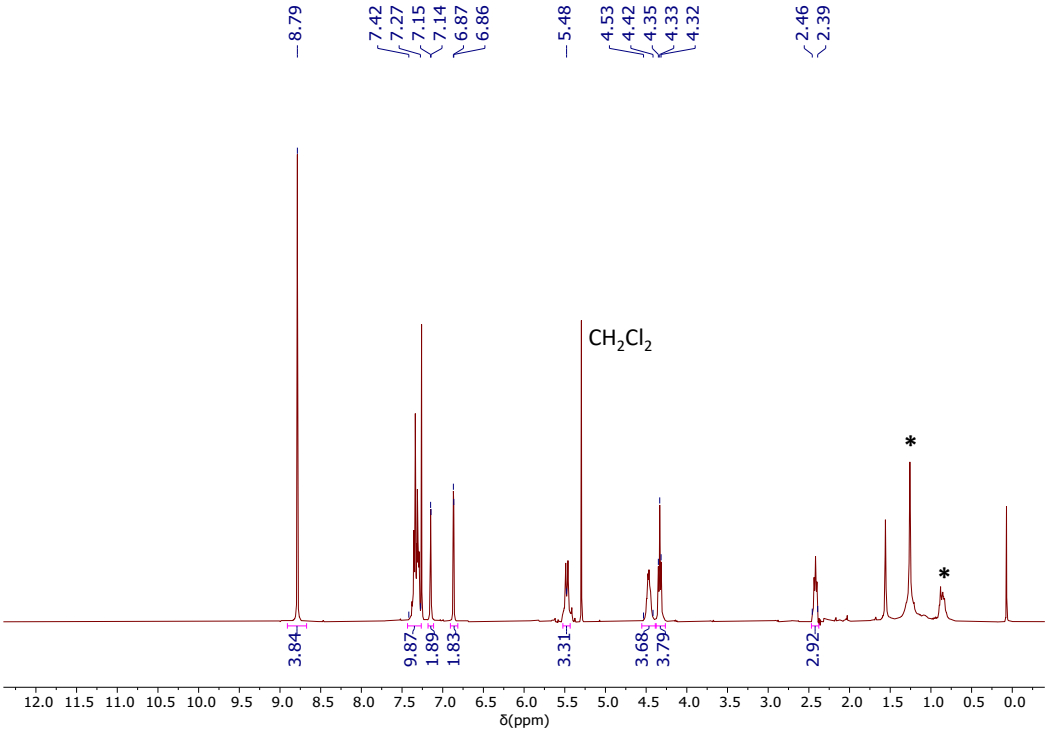

Figure S15. ^{1}H NMR spectrum (400 MHz, $CDCl_3$) of **4B**

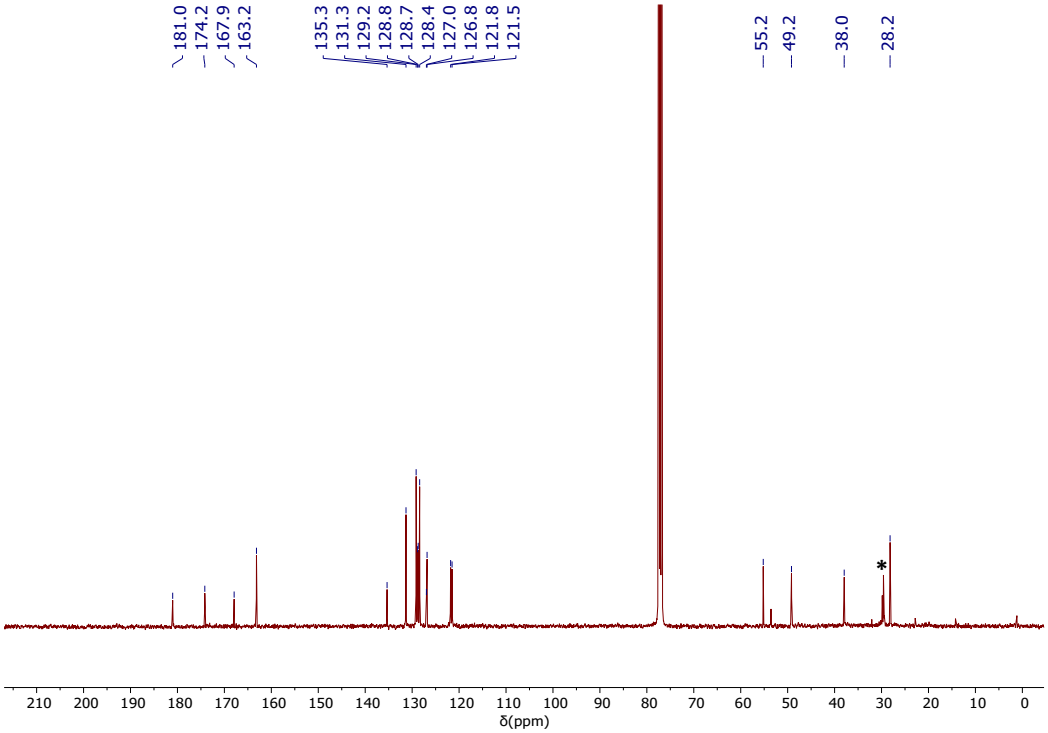

Figure S16. $^{13}C\{^{1}H\}$ spectrum (101 MHz, $CDCl_3$) of **4B**

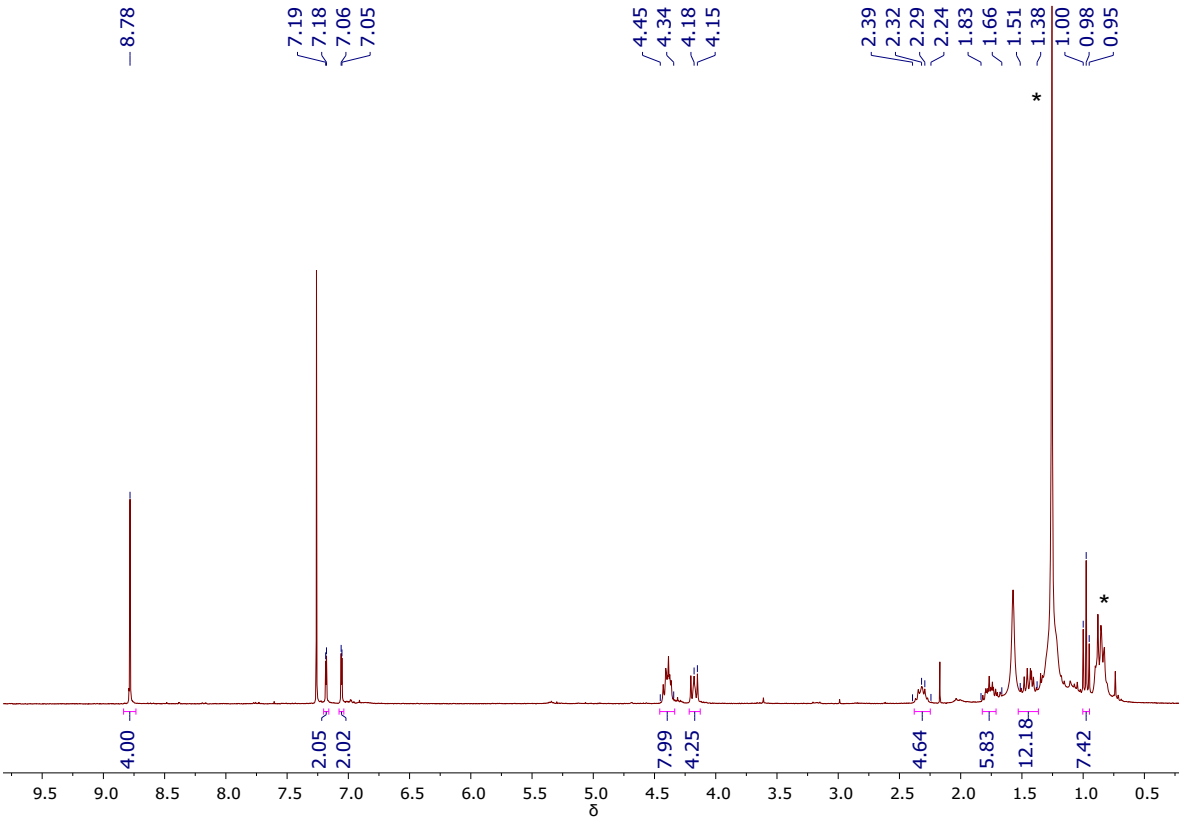

Figure S17. ^{1}H NMR spectrum (400 MHz, $CDCl_3$) of **5**

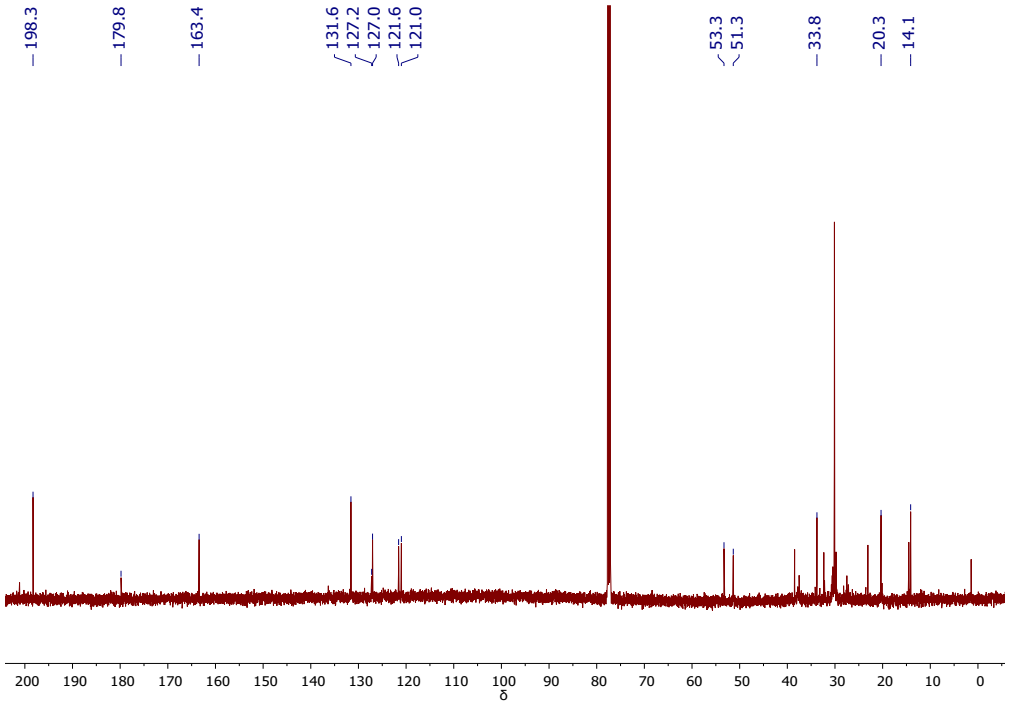

Figure S18. $^{13}C\{^{1}H\}$ spectrum (125 MHz, $CDCl_3$) of **5.**

3. X-ray crystallography

X-Ray Diffraction studies for complex 3B. Single crystals for X-Ray studies of **3B** were obtained by slow evaporation of a concentrated solution of the complex in chloroform. Diffraction data was collected on an Agilent SuperNova diffractometer equipped with an Atlas CCD detector using Cu-Kα radiation (λ = 1.54184 Å). Single crystals were mounted on a MicroMount® polymer tip (MiteGen) in a random orientation. Absorption corrections based on Gaussian methods. Using Olex2,[4] the molecular structure of the compound was solved by Charge Flipping in Superflip,[5] and refined by least squares with the ShelXL refinement package.[6] Key details of the crystals and structure refinement data are summarized in Supplementary Table S1. Further crystallographic details may be found in the CIF files, which were deposited at the Cambridge Crystallographic Data Centre, Cambridge, UK. The reference number for complex **3B** was assigned as 2170148.

Table S1. Summary of crystal data, data collection, and structure refinement details of **3B**

	3B		**3B**
Empirical formula	$C_{58}H_{56}Cl_8Ir_2N_6O_4$	**ρ_{calc} g/cm^3**	1.294
Formula weight	1569.08	**μ/mm^{-1}**	9.053
Temperature/K	200.1(9)	**F(000)**	3072.0
Crystal system	monoclinic	**Crystal size/mm^3**	0.18 × 0.064 × 0.049
Space group	C2/c	**2Θ range for data collection/°**	7.806 to 133.198
a/Å	26.1313(9)	**Index ranges**	-31 ≤ h ≤ 29, -21 ≤ k ≤ 21, -16 ≤ l ≤ 19
b/Å	18.4166(6)	**Reflections collected**	40535
c/Å	16.7444(5)	**Independent reflections**	7102 [R_{int} = 0.0692, R_{sigma} = 0.0335]
α/°	90	**Data/restraints/parameters**	7102/351/388
β/°	92.392(3)	**Goodness-of-fit on F^2**	1.087
γ/°	90	**Final R indexes [I>=2σ (I)]**	R_1 = 0.0577, wR_2 = 0.1894
Volume/Å^3	8051.2(5)	**Final R indexes [all data]**	R_1 = 0.0682, wR_2 = 0.2028
Z	4	**Largest diff. peak/hole / e Å^{-3}**	1.78/-1.31

4. Photophysical properties

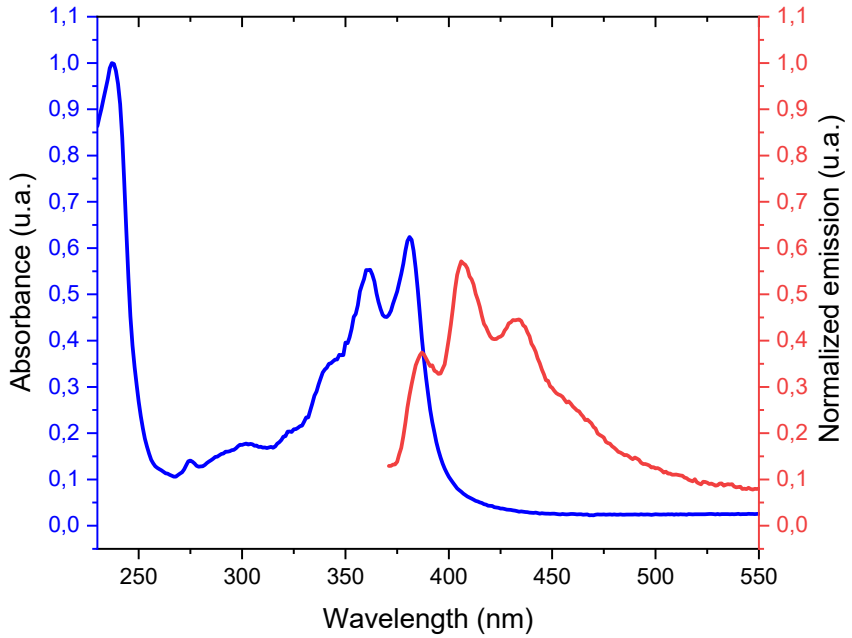

Figure S19. UV-Vis and emission spectra (λ_{exc} = 361 nm) of complex [**1A**](Br)$_2$, recorded in CH_2Cl_2 at a concentration of 1.0x10^{-5} M.

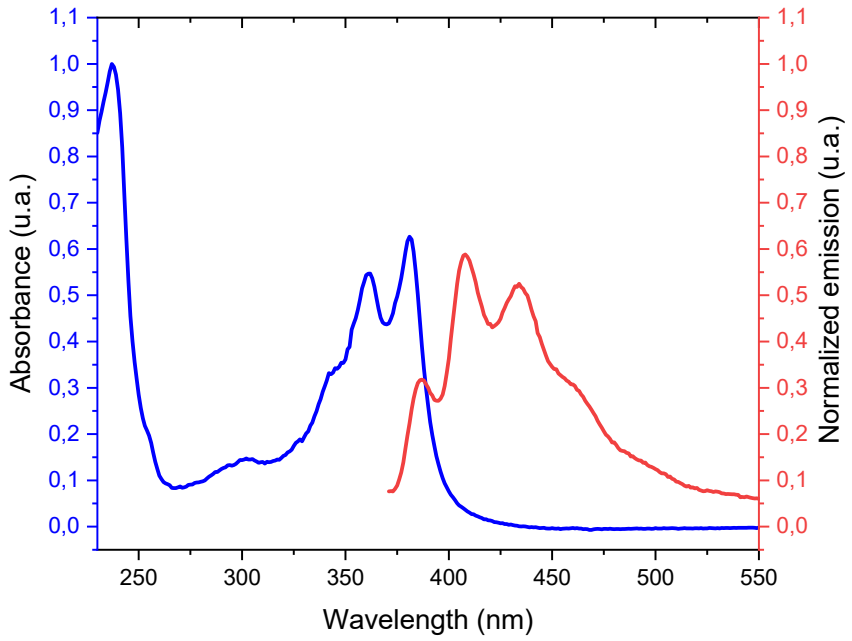

Figure S20. UV-Vis and emission spectra (λ_{exc} = 361 nm) of complex [**1B**](Br)$_2$, recorded in CH_2Cl_2 at a concentration of 2.0x10^{-5} M

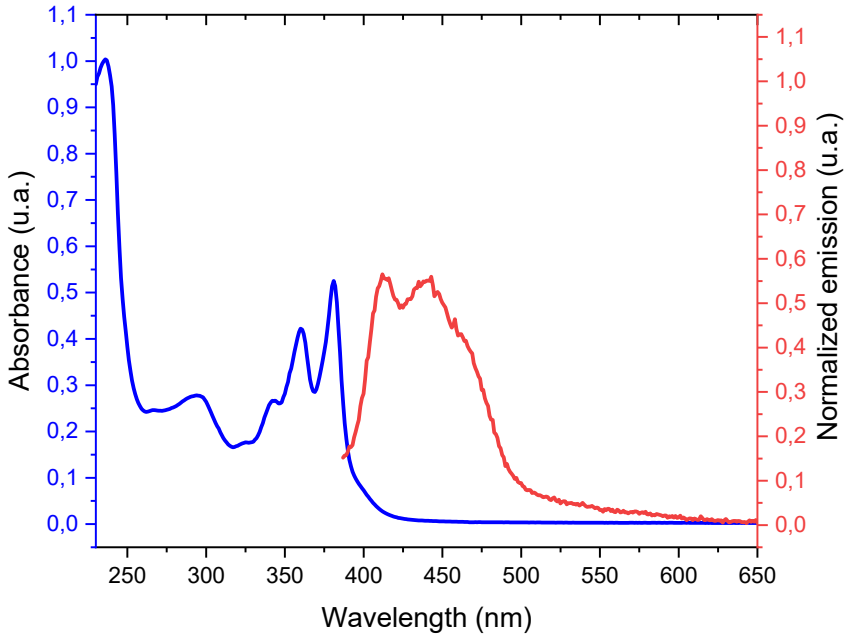

Figure S21. UV-Vis and emission spectra (λ_{exc} = 361 nm) of complex **2A**, recorded in CH_2Cl_2 at a concentration of 2.0×10^{-5} M

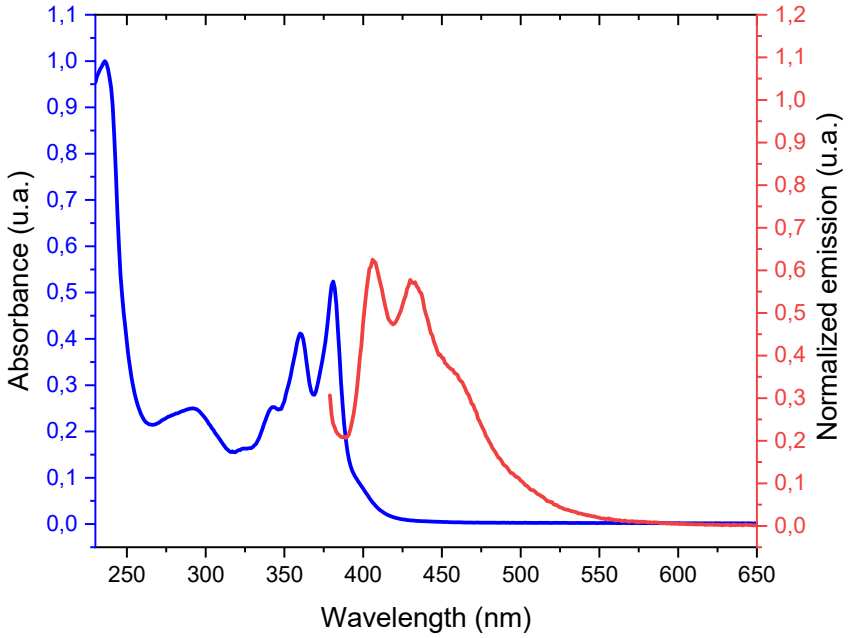

Figure S22. UV-Vis and emission spectra (λ_{exc} = 361 nm) of complex **2B**, recorded in CH_2Cl_2 at a concentration of 2.0×10^{-5} M

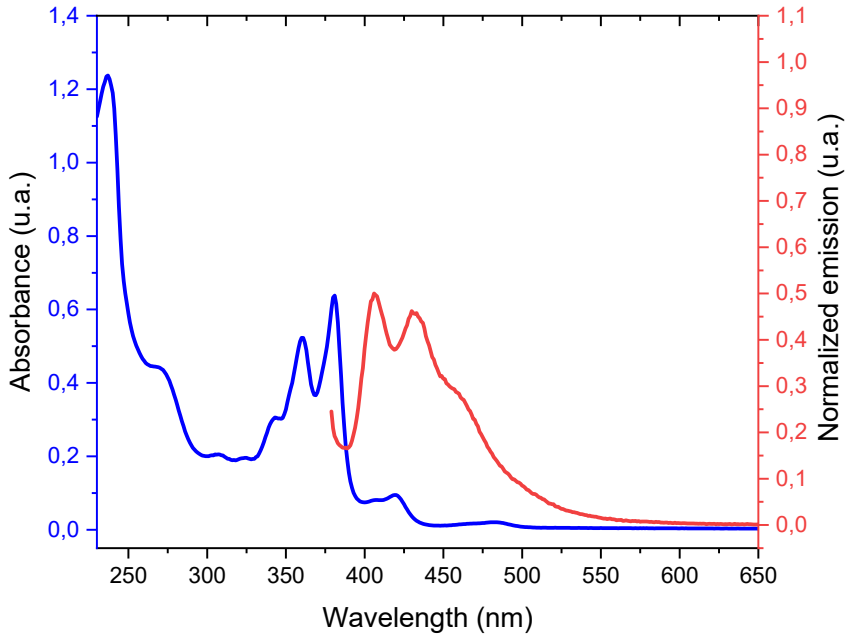

Figure S23. UV-Vis and emission spectra (λ_{exc} = 361 nm) of complex **3A**, recorded in CH_2Cl_2 at a concentration of 2.0×10^{-5} M

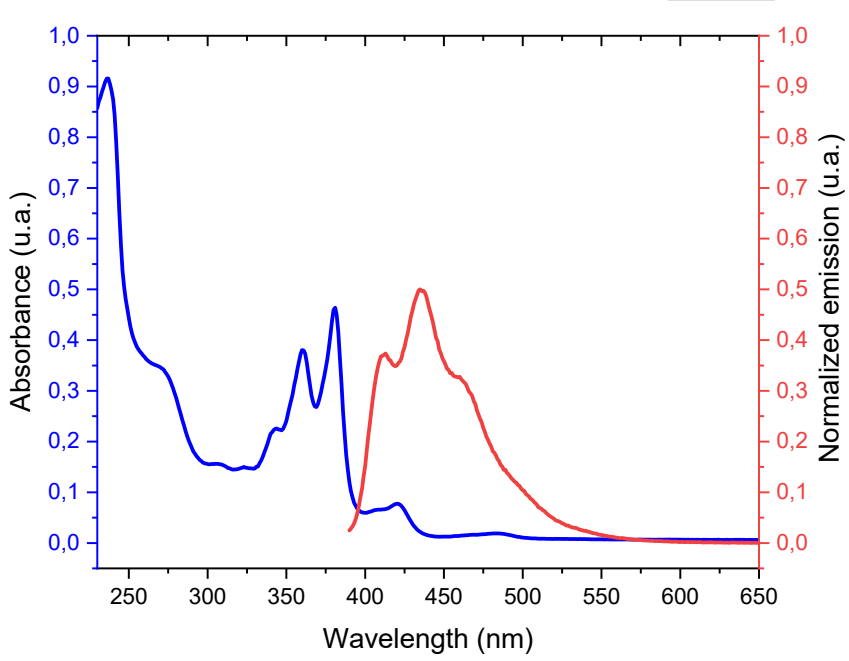

Figure S24. UV-Vis and emission spectra (λ_{exc} = 361 nm) of complex **3B**, recorded in CH_2Cl_2 at a concentration of 2.0×10^{-5} M

Table S2. Summary of the photophysical properties of the NDI-derived compounds[a]

Compound	λ_{abs} [nm]	λ_{NDI} [nm]	$\lambda_{em,\ max}$ [nm]
[**1A**]$(Br)_2$	237.0, 361.0, 381.0	362.0, 381.0	406.0
[**1A**]$(Br)_2$	237.1, 362.5, 381.0	362.5, 381.0	408.0
2A	236.3, 294.1, 343.1, 360.4, 381.0	360.4, 381.0	411.9
2B	236.1, 291.4, 343.0, 360.4, 380.9	360.4, 380.9	405.9
3A	236.6, 343.6, 360.4, 380.7, 419.2	360.4, 380.7	406.9
3B	236.3, 343.4, 360.5, 380.7, 420.6	360.5, 380.7	435.0

[a]Measurements were performed in dry and degassed CH_2Cl_2 under ambient conditions

5. Electrochemical studies

5.1. Electrochemical measurements

Electrochemical studies were carried out by using an Autolab Potentiostat, Model PGSTAT101 and three-electrode cell, controlled with NOVA 2.1.4 software. The cell was equipped with platinum working and counter electrodes, as well as a silver wire pseudoreference electrode. In all experiments, $[N(nBu)_4][PF_6]$ (0.1M in dry CH_2Cl_2) was used as the supporting electrolyte with an analyte concentration of approximately 1 Mm. Measurements were performed at 25, 50, 100, 250 and 500 mV/s scan rates. All scans were referenced to the ferrocenium/ferrocene (Fc^+/Fc) couple at 0 V. Ohmic drop was minimized by minimizing the distance between the working and reference electrodes. The residual ohmic drop was estimated by positive feedback and compensated at 85%.

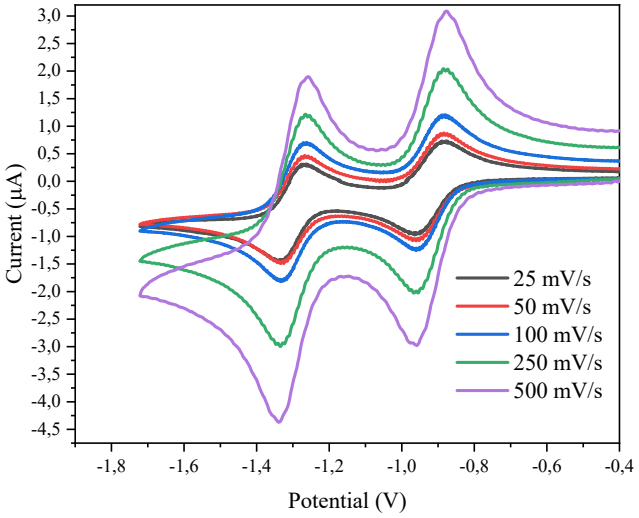

Figure S25. Cyclic voltammogram of [**1A**](Br)$_2$ at different scan rates

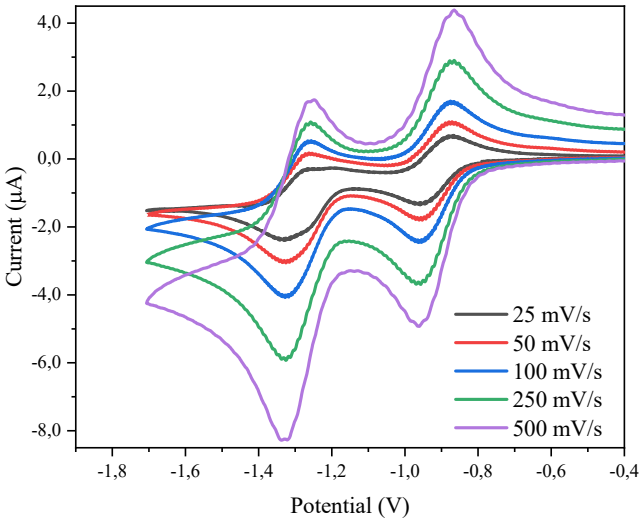

Figure S26. Cyclic voltammogram of [**1B**](Br)$_2$ at different scan rates

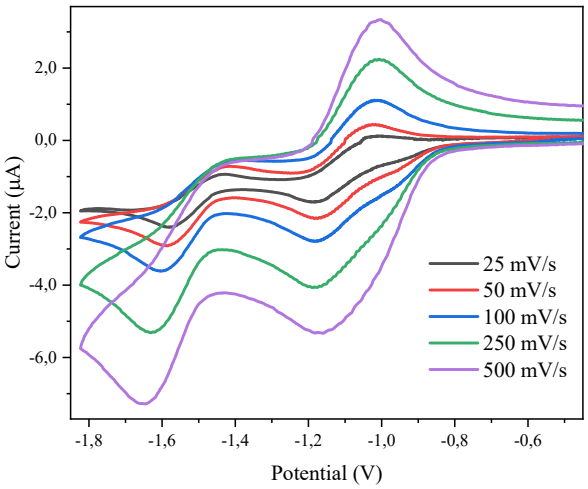

Figure S27. Cyclic voltammogram of **2A** at different scan rates

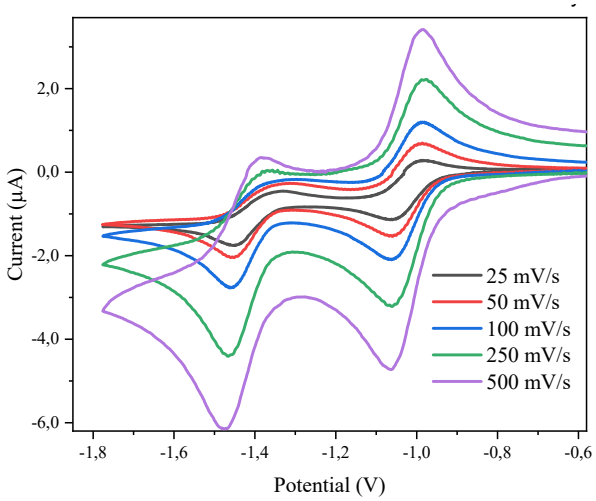

Figure S28. Cyclic voltammogram of **2B** at different scan rates

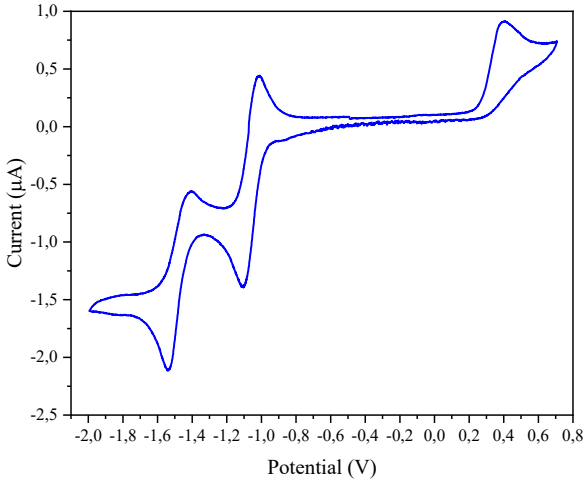

Figure S29. Cyclic voltammogram of **2A** at 25 mV/s scan rate showing the irreversible oxidation wave

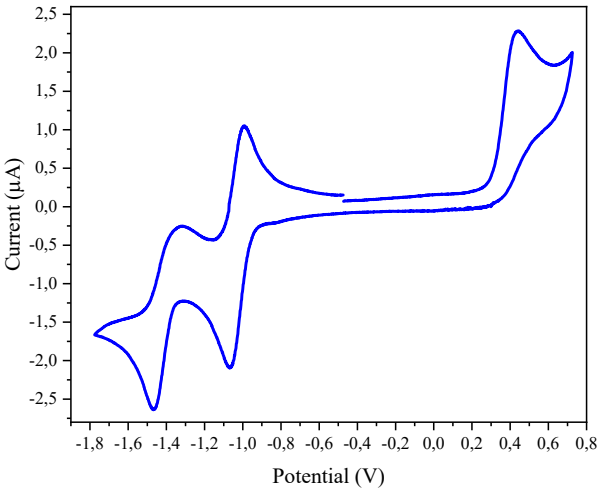

Figure S30. Cyclic voltammogram of **2B** at 100 mV/s scan rate showing the irreversible oxidation wave

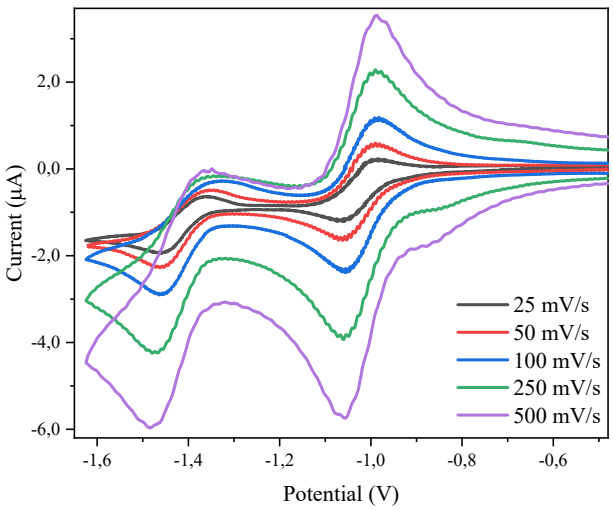

Figure S31. Cyclic voltammogram of **3A** at different scan rates

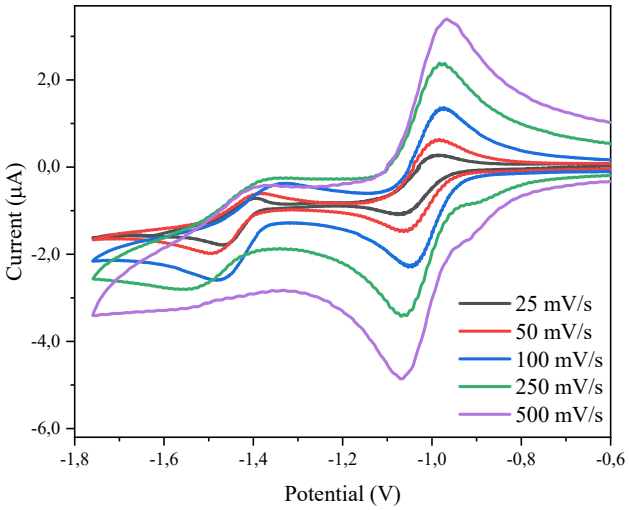

Figure S32. Cyclic voltammogram of **3B** at different scan rates

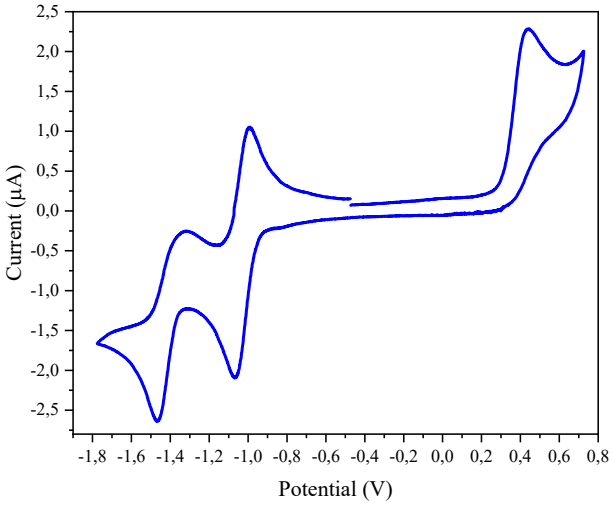

Figure S33. Cyclic voltammogram of **3A** at 100 mV/s scan rate showing the irreversible oxidation wave

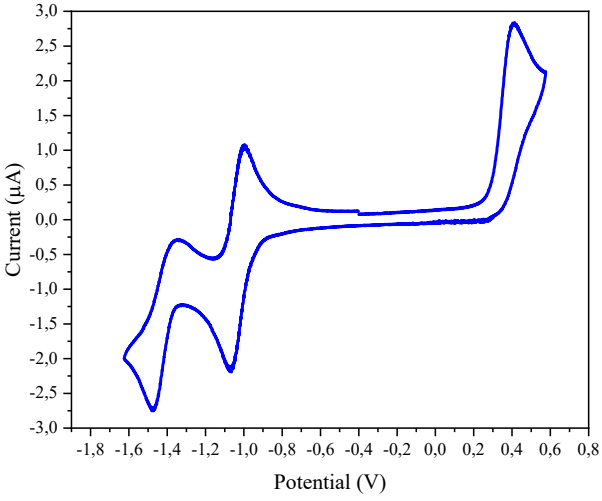

Figure S34. Cyclic voltammogram of **3B** at 100 mV/s scan rate showing the irreversible oxidation wave

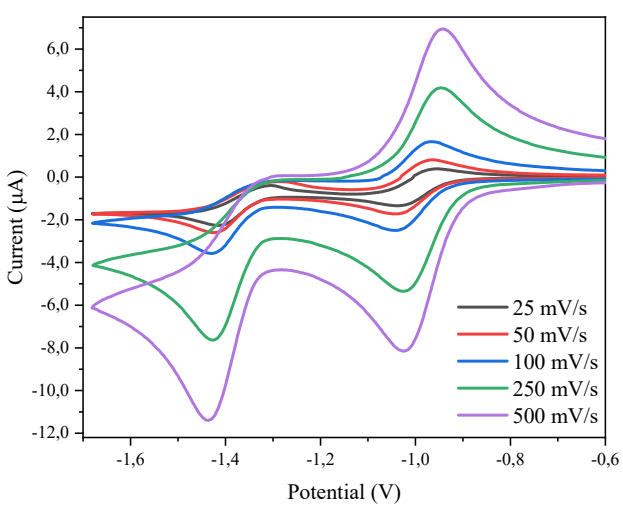

Figure S35. Cyclic voltammogram of **4A** at different scan rates

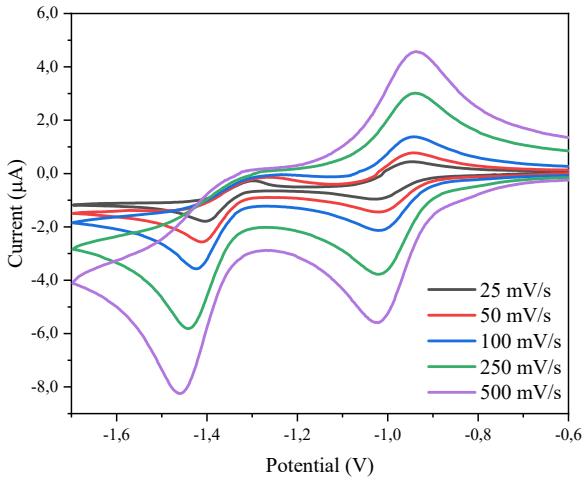

Figure S36. Cyclic voltammogram of **4B** at different scan rates

Table S3. Electrochemical properties of compounds **1**, **2**, **3** and **4**[a]

Compound	$E^2_{1/2}$ (V)/ΔE (mV)[b]	$E^1_{1/2}$ (V)/ΔE (mV)	E_{pa} (V)[c]
[**1A**](Br)$_2$	-1.30/71	-0.92/75	-
[**1B**](Br)$_2$	-1.29/71	-0.92/91	-
2A	-1.53	-1.06/91	0.39
2B	-1.47	-1.03/77	0.45
3A	-1.44	-1.03/77	0.44
3B	-1.49	-1.02/79	0.43
4A	-1.42	-1.00/78	-
4B	-1.41	-0.97/81	-

[a]Measurements performed at a scan rate of 100 mVs^{-1} and referenced *vs.* ferrocenium/ferrocene. [b]The second reduction event is an irreversible process for complexes **2**, **3** and **4**, the value indicated in the table corresponds to the cathodic peak potential (E_{pc}). [c]The oxidation event is an irreversible process for complexes **2** and **3**, the value indicated in the table corresponds to the anodic peak potential (E_{pa}).

5.2 Spectroelectrochemical measurements

Spectroelectrochemical (SEC) measurements were performed using a gastight, optically transparent thin-layer solution cell fabricated by Prof. Hartl at the University of Reading (Reading, U.K.), as described previously.[7] The SEC cell contained a masked Au-minigrid working electrode (32 wires/cm), a Pt-gauze auxiliary electrode, and an Ag-wire pseudo-reference electrode and had CaF_2 windows. In each experiment, electrochemical reduction of the species of interest ([Analyte] = 3 mM for IR experiments and 0.25 mM for UV-vis experiments, $[N(nBu)_4][PF_6]$ = 250 mM in CH_2Cl_2 (under nitrogen atmosphere)).

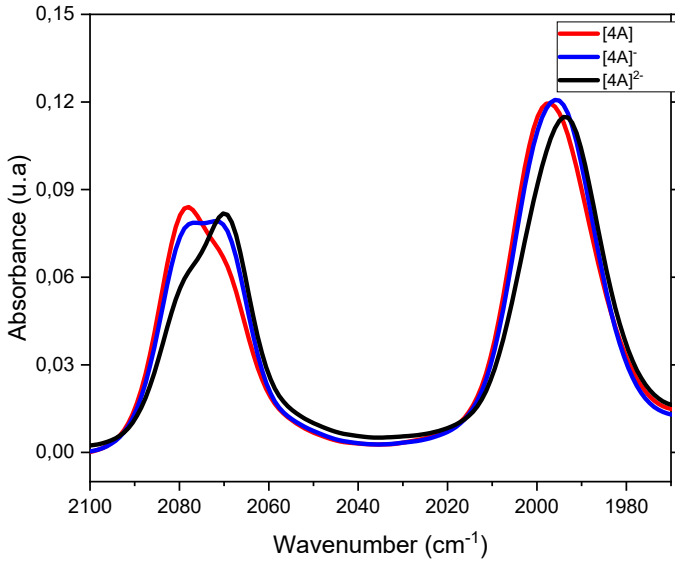

Figure S37. IR-SEC monitoring of the reduction of **4A** in CH_2Cl_2. Lines represent the spectra of the starting (red), singly-reduced (blue) and doubly-reduced (black) species.

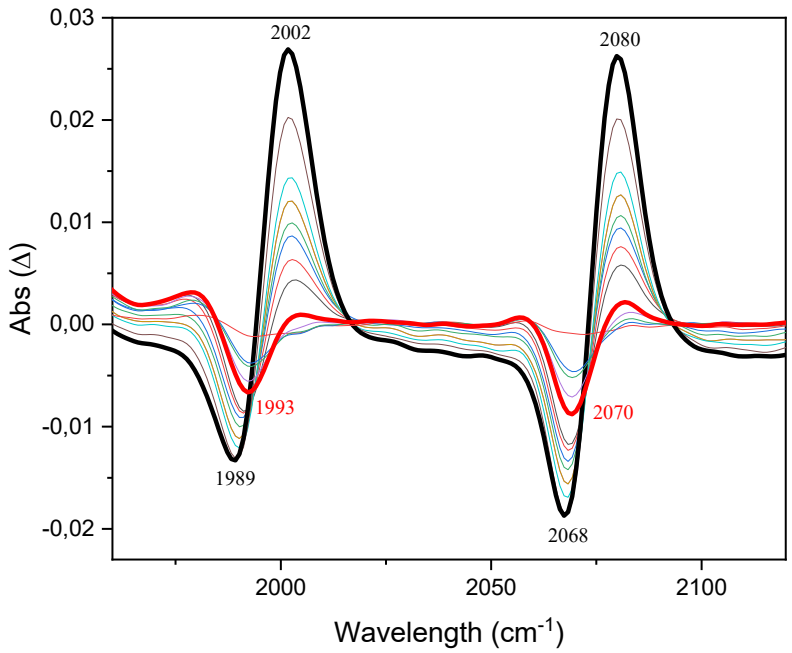

Figure S38. Infrared difference spectra resulting from the IR-SEC reduction of **4A** in CH_2Cl_2. The electrochemical reduction was performed applying progressively lower potentials with a Au working electrode, Pt counter electrode, and Ag wire pseudo-reference electrode.

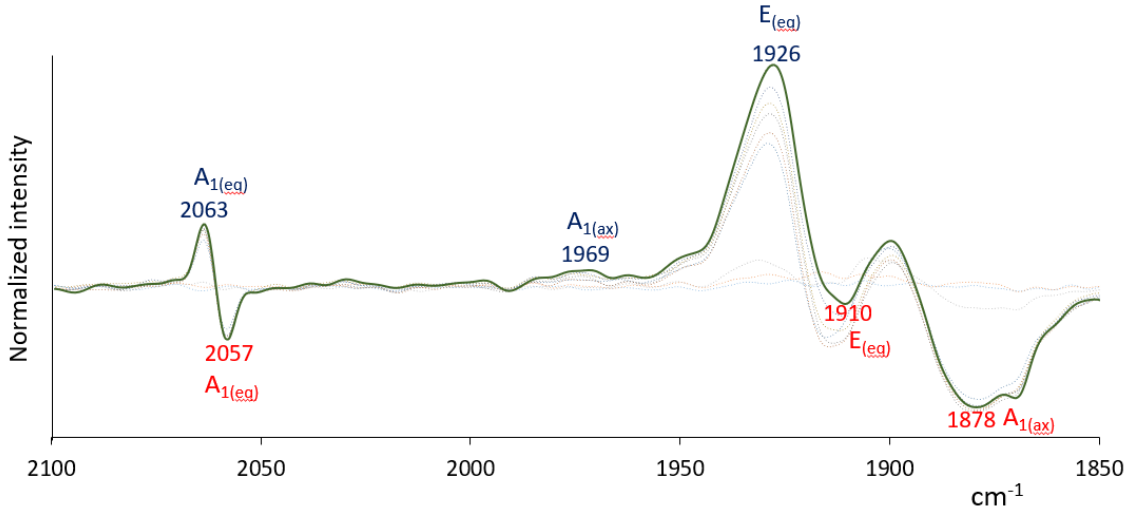

Figure S39. IR difference spectra resulting from the IR-SEC reduction of $[NDI\text{-}(NHC)_2][W(CO)_5]_2$ in CH_2Cl_2 (0.25 M $[N(nBu)_4][PF_6]$). The electrochemical reduction was performed applying progressively lower potentials with a Au working electrode, Pt counter electrode, and Ag wire pseudo-reference. The frequencies in blue refer to the neutral complex, while those in red are due to the doubly-reduced complex.

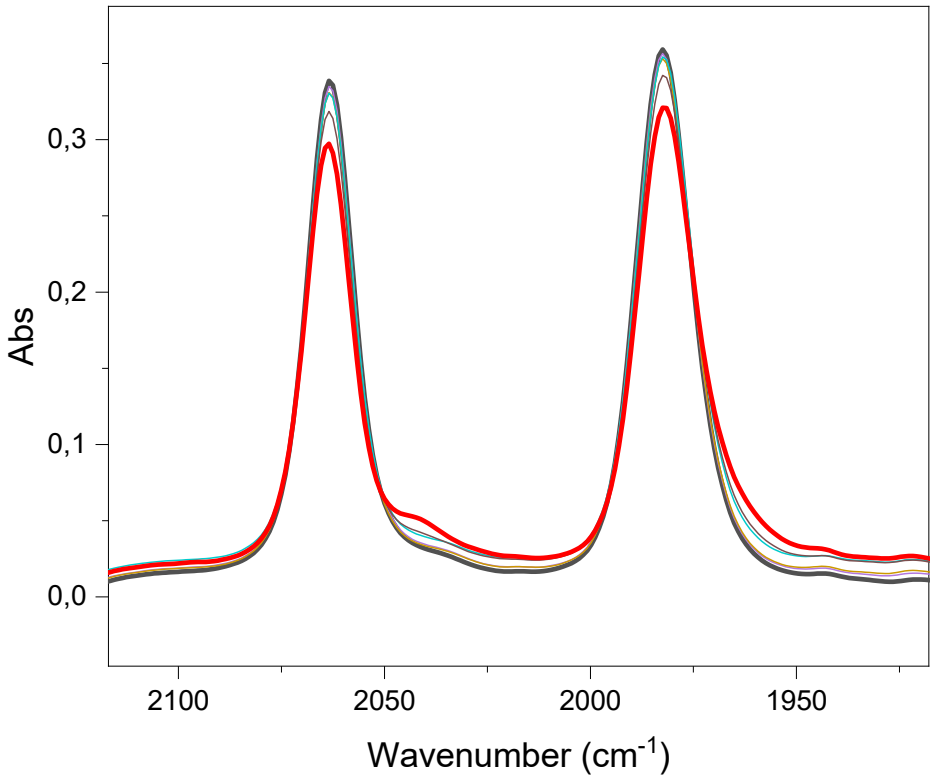

Figure S38. FT-IR spectra resulting from the IR-SEC reduction of [IrCl(IBu)$(CO)_2$] (IBu =1,3-di-n-butylimidazole-2-ylidene) (5mM) and N,N'-dibutyl-1,4,5,8-naphthalenetetracarboxylic acid diimide (5mM) in CH_2Cl_2 ($TBAPF_6$ 0.25M). The electrochemical reduction was performed applying progressively lower potentials with a Au working electrode, Pt counter electrode, and Ag wire pseudo-reference electrode.

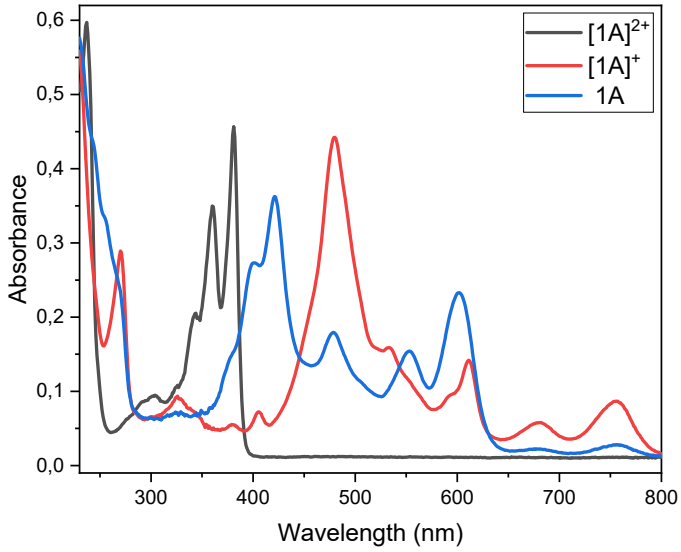

Figure S38. UV-vis SEC monitoring of the reduction of salt [**1A**](Br)$_2$ in CH_2Cl_2. Lines represent the spectra of the starting (black), singly-reduced (red) and doubly-reduced (blue) species.

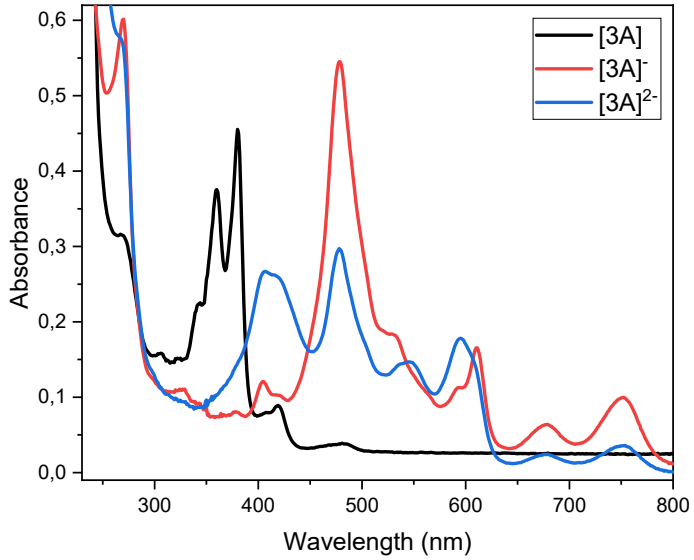

Figure S39. UV-vis SEC monitoring of the reduction of **3A** in CH_2Cl_2. Lines represent the spectra of the starting (black), singly-reduced (red) and doubly-reduced (blue) species.

6. Catalytic studies: cyclization of acetylenic carboxylic acids

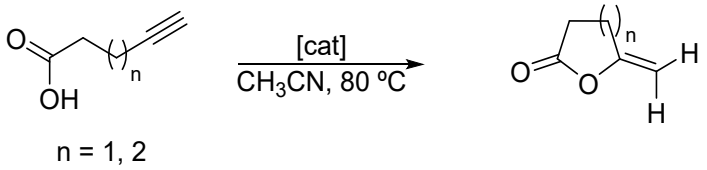

n = 1, 2

All the catalytic experiments and manipulations were conducted under nitrogen atmosphere. Complex $[Fe(\eta_5\text{-}C_5H_4COMe)Cp][BF_4]$[8] was prepared according to the literature procedure. All other reagents were purchased from commercial sources and used as received. For this study, complexes **2A** and **3A** were employed as model catalysts.

Cyclization of 4-pentynoic acid to γ-methylene-γ-butyrolactone. In a high pressure Schlenk tube fitted with a Teflon cap, the corresponding catalyst (0.05 mol % to 0.4 mol % based on metal) was added to a 0.33 M solution of 4-pentynoic acid (0.5 mmol) and 1,3,5-trimethoxybenzene (0.5 mmol) in CD_3CN. The mixture was heated at 80 °C. Yields were determined by ^{1}H-NMR spectroscopy using 1,3,5-trymethoxybenzene as internal standard. γ-Methylene-γ-butyrolactone was isolated as the only product. Spectroscopic data were consistent with those reported in the literature. ^{1}H NMR (400 MHz, CD_3CN): δ 4.65-4.63 (m, 1H, C=CH_2), 4.30-4.28 (m, 1H, C=CH_2), 2.88-2.83 (m, 2H, CH_2), 2.65-2.61 (m, 2H, CH_2).

Cyclization of 5-hexynoic acid to 6-methylidenetetrahydro-2-pyrone. In a high pressure Schlenk tube fitted with a Teflon cap, the corresponding catalyst (0.1 mol % or 1 mol % based on metal) was added to a 0.083 M solution of 5-hexynoic acid (0.125 mmol) and 1,3,5-trimethoxybenzene (0.125 mmol) in CD_3CN. The mixture was heated at 80 °C. Yields were determined by ^{1}H NMR spectroscopy using 1,3,5-trymethoxybenzene as internal standard. 6-Methylidenetetrahydro-2-pyrone, was obtained as the only product. Spectroscopic data were consistent with those reported in the literature. ^{1}H NMR (400 MHz, CD_3CN): δ 4.56-4.57 (m, 1H, C=CH_2), 4.32-4.30 (m, 1H, C=CH_2), 2.60 (t, 2H, $^2J_{H\text{-}H}$ = 6.8 Hz, CH_2), 2.52-2.48 (m, 2H, CH_2), 1.87-1.80 (m, 2H, CH_2).

Table S4 shows the rate constants calculated by plotting the concentration of the product (γ-methylene-γ-butyrolactone) *versus* time, assuming a zero order reaction with respect to substrate, at different catalyst (**2A**) loadings (Figure S39). Figure S40 shows the plot of the

initial rates *versus* the concentrations of catalyst **2A** that allows to calculate a first reaction order in catalyst.

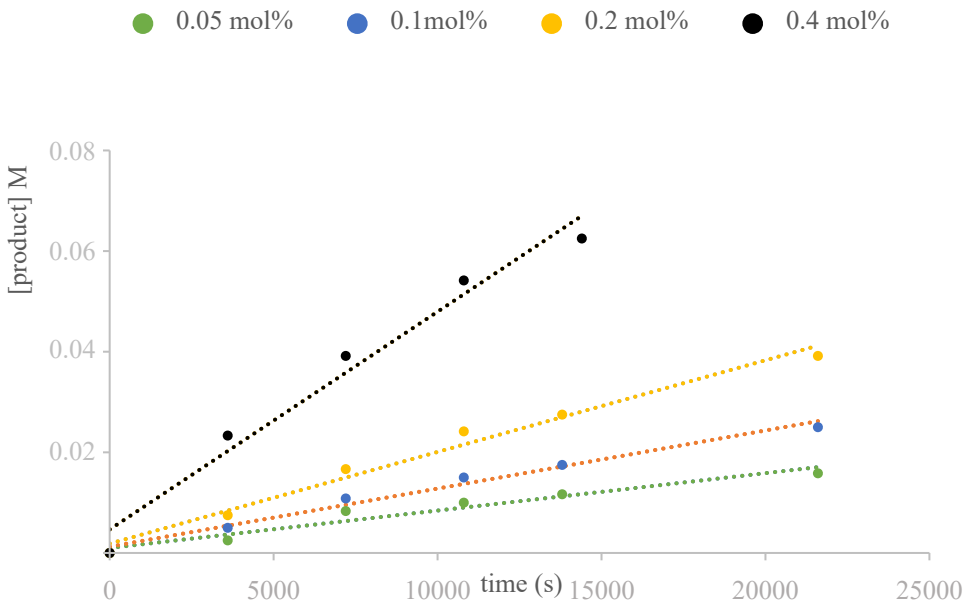

Figure S40. Formation of the product (γ-methylene-γ-butyrolactone) over time varying the catalyst (**2A**) loading assuming zero order reaction.

Table S4. Rate constants assuming zero order reaction

Entry	Catalyst loading (mol% Rh)	Rate constants (*10^{-6} Ms^{-1})
1	0.05	1.49
2	0.10	2.31
3	0.20	3.64
4	0.40	8.66

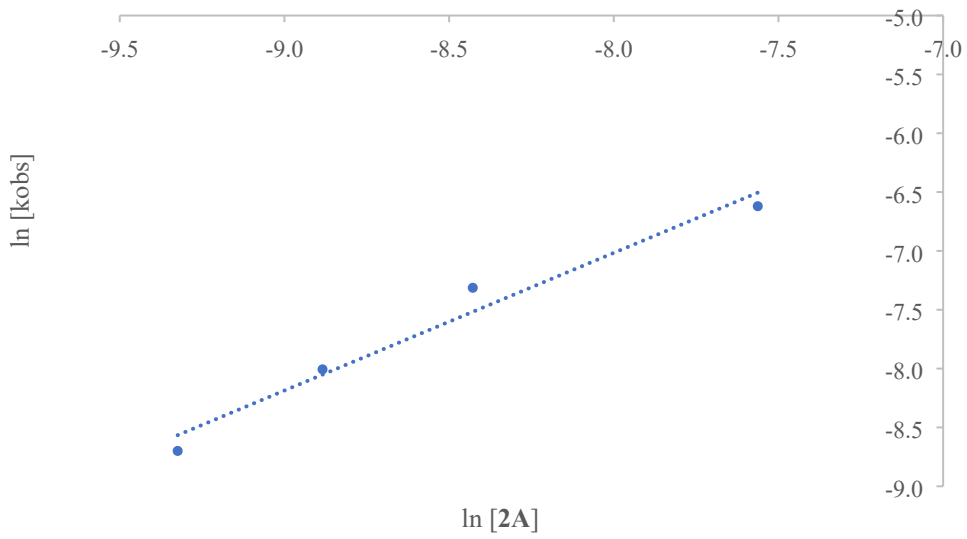

Figure S41. Dependence of the ln of the rate constants on the ln of catalyst (**2A**) concentration. Determination of the order with respect to catalyst **2A**.

Reactivity of the catalysts in the presence of cobaltocene and decamethylcobaltocene. The experiments were carried out as explained above for the cyclization of 4-pentynoic and 5-hexynoic acids, adding 1.3 equivalents of cobaltocene ([$CoCp_2$]) to the reaction mixture. The evolution of the reaction was monitored by ^{1}H NMR spectroscopy collecting a small aliquot at the desired times, using 1,3,5-trymethoxybenzene as internal standard. Figure S41 plots the time-dependent reaction profiles for the cyclization of 4-pentynoic acid in the presence of 0.1 mol% of **2A** with and without cobaltocene. Figure S42 plots the time-dependent reaction profiles for the cyclization of 5-hexynoic acid in the presence of 1 mol% of **3A** with and without cobaltocene.

In two independent experiments, the cyclization of 4-pentynoic and 5-hexynoic acids was carried out using **3A** and 2.3 equivalents of decamethylcobaltocene ([$CoCp^*_2$]). The reactions were allowed to evolve for the desired times. The product yields are shown in Table S5. The data shown allows a comparison of the catalytic behavior of **3A** in the absence of any redox additive, and in the presence of [$CoCp_2$] and [$CoCp^*_2$].

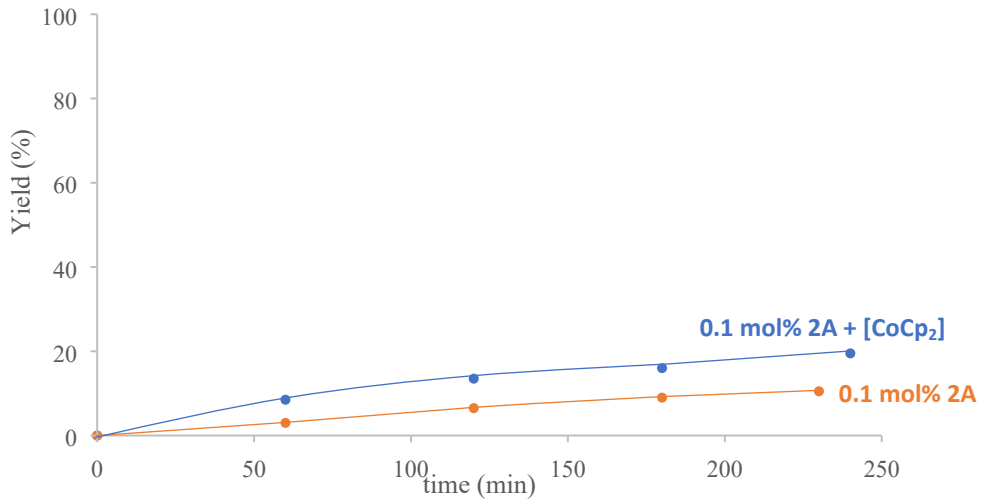

Figure S42. Time-dependent reaction profiles for the cyclization of 4-pentynoic acid in the presence of 0.1 mol% of **2A** with (blue) and without (orange) addition of cobaltocene. The reactions were carried out in CD_3CN, with an initial concentration of 4-pentynoic acid of 0.33 M.

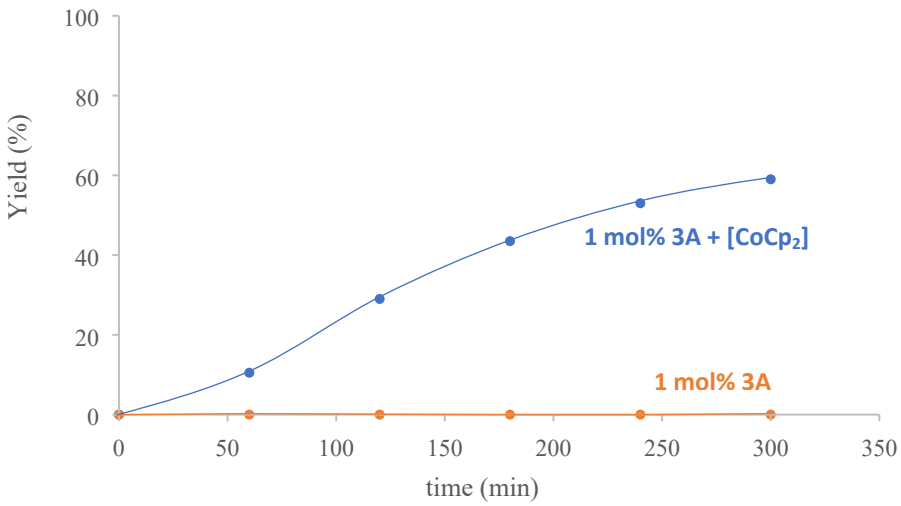

Figure S43. Time-dependent reaction profile for the cyclization of 5-hexynoic acid in the presence of 1 mol% of **3A** with (blue line) and without (orange line) addition of cobaltocene. The reactions were carried out in CD_3CN, with an initial concentration of 5-hexynoic acid of 0.083 M.

Redox switching experiments. In a high pressure Schlenk tube fitted with a Teflon cap, complex **3A** (0.1 mol % based on metal) was added to a 0.33 M solution of 4-pentynoic acid (0.5 mmol) and 1,3,5-trimethoxybenzene (0.5 mmol) in CD_3CN. The mixture was heated at 80 °C. The reaction was monitored for 2 hours collecting a small aliquot at the desired times. The reductant cobaltocene was then added to the reaction mixture under nitrogen. After collecting data for 60 minutes, 1.5 equivalent (with respect to the catalyst) of a chemical oxidant, namely $[Fe(\eta_5\text{-}C_5H_4COCH_3)Cp][BF_4]$ ([Fc'](BF_4])), was added to the reaction mixture under nitrogen. The reaction was monitored for further 180 minutes collecting a small aliquot at the desired times. The evolution of the reaction was monitored by ^1H NMR using 1,3,5-trymethoxybenzene as internal standard.

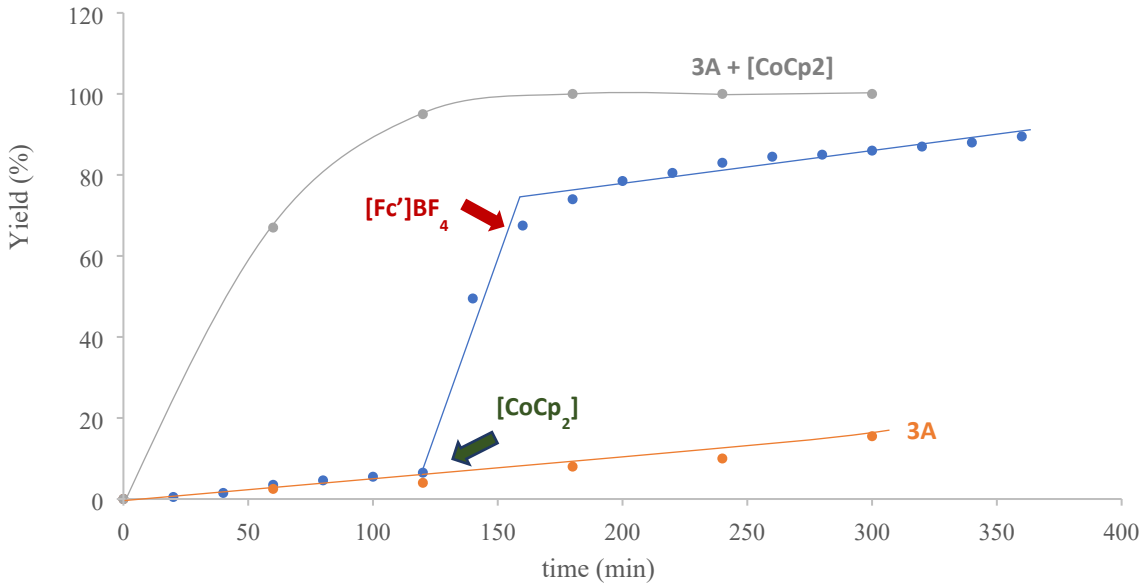

Figure S44. Plot showing the cyclization of 4-pentynoic acid with 0.1 mol% of **3A** and sequential additions of [Cp_2Co] and acetyl ferrocenium tetrafluoroborate, [Fc'](BF_4) (blue solid dots). The plots showing the evolution of the reaction using 0.1 mol% of **3A** (orange solid dots) and **3A**+ [$CoCp_2$] (grey solid dots) are also shown for comparison.

Table S5. Cyclization of 4-pentynoic and 5-pentynoic acids using **3A** as catalyst.

Entry	Alkynoic Acid	Cat. Load (Mol%)	Additive	t [h]	Yield [%]
1	4-pentynoic	0.1	none	5	15.5
2	4-pentynoic	0.1	[$CoCp_2$]	2.5	>99.0
3	4-pentynoic	0.1	[$CoCp^*_2$]	7	73
4	5-hexynoic	1	none	24	<1.0
5	5-hexynoic	1	[$CoCp_2$]	5	60
6	5-hexynoic	1	[$CoCp_2$]	7	82
7	5-hexynoic	1	[$CoCp^*_2$]	7	48

[a]The reactions were carried out in acetonitrile at 80ºC, with an initial concentration of 4-alkynoic acid of 0.33 M. The amount of cobaltocene and decamethylcobaltocene was 1.3 or 2.3 equivalents with respect to **3A**, respectively. Yields were determined by ^{1}H-NMR spectroscopy, using 1,3,5-trimethoxybenzene as integration standard.

7. References

1. A. Kalita, S. Hussain, A. H. Malik, U. Barman, N. Goswami and P. K. Iyer, *ACS Appl. Mater. Interfaces*, 2016, **8**, 25326-25336.
2. P. K. R. Panyam and T. Gandhi, *Adv. Synth. Catal.*, 2017, **359**, 1144-1151.
3. G. R. Fulmer, A. J. M. Miller, N. H. Sherden, H. E. Gottlieb, A. Nudelman, B. M. Stoltz, J. E. Bercaw and K. I. Goldberg, *Organometallics*, 2010, **29**, 2176-2179.
4. O. V. Dolomanov, L. J. Bourhis, R. J. Gildea, J. A. K. Howard and H. Puschmann, *J. Appl. Crystallogr.*, 2009, **42**, 339-341.
5. L. Palatinus and G. Chapuis, *J. Appl. Crystallogr.*, 2007, **40**, 786-790.
6. G. M. Sheldrick, *Acta Crystallogr. A*, 2015, **71**, 3-8.
7. H. L. Wang, L. C. Chen and Y. Xiao, *J. Mater. Chem. C*, 2017, **5**, 8875-8882.
8. N. G. Connelly and W. E. Geiger, *Chem. Rev.*, 1996, **96**, 877-910.